

# Ionospheric Irregularities Across African Sector: Observation Perspective

*J. Olwendo<sup>1</sup> & P. J. Cilliers<sup>2</sup>*

<sup>1</sup>Pwani University, Department of Physics, Box 195-80108, Kilifi-Kenya,

<sup>2</sup>South African National Space Agency, Space Science Directorate,  
Hermanus, South Africa,

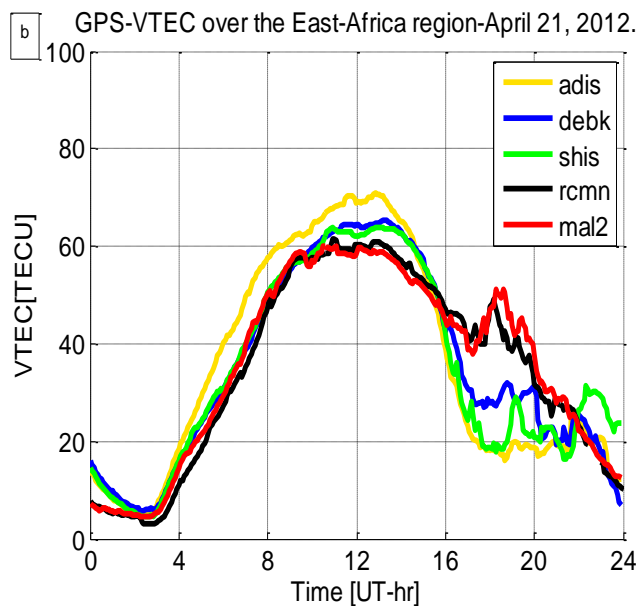
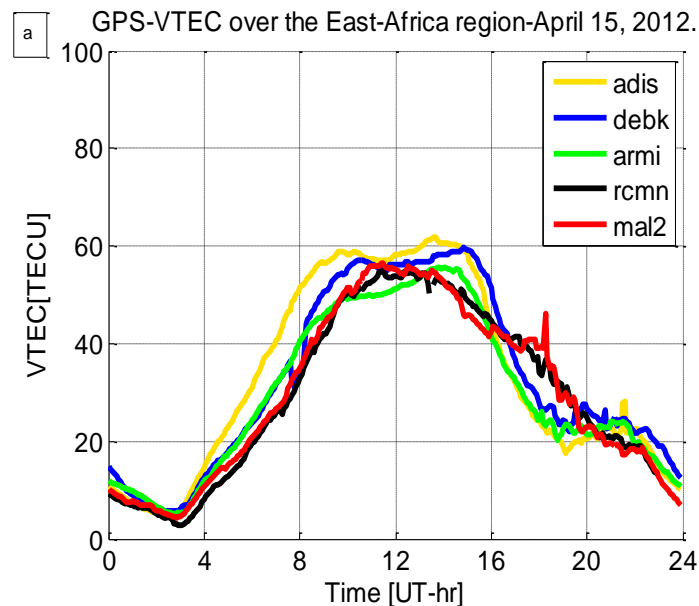
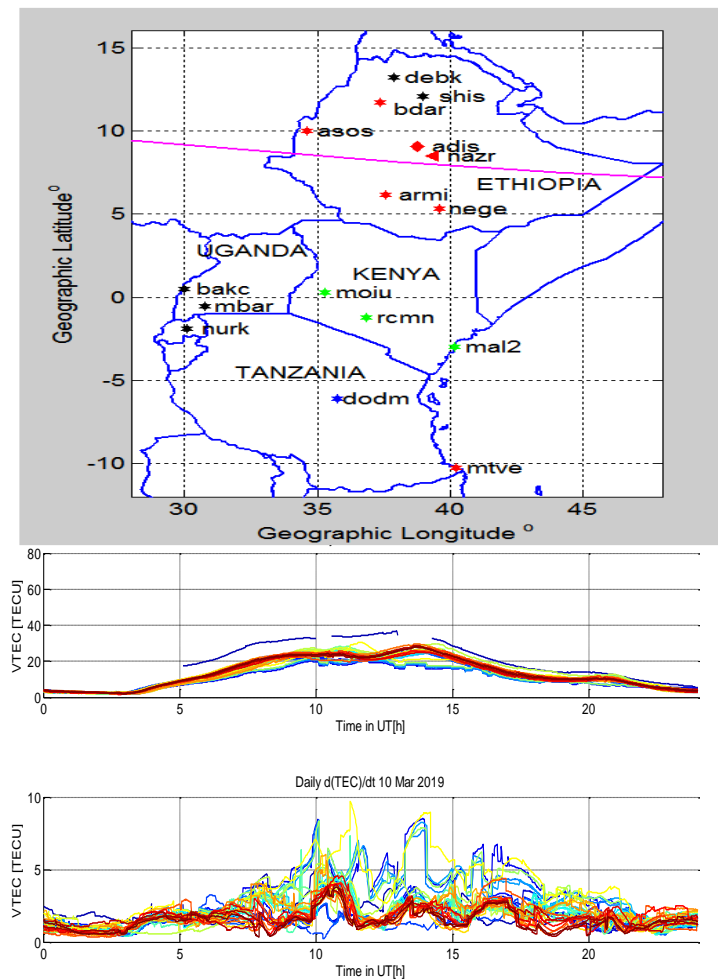


**2<sup>ND</sup> Eastern Africa Global Navigation Satellite System and Space weather Capacity Building workshop, 21<sup>st</sup> -25<sup>th</sup>, June, 2021. Pwani University/Trieste (Kenya/Italy).**

# Outline

- ❖ **Diurnal variation of Ionosphere: Smooth Ionosphere**
- ❖ **Ionospheric Irregularities and why it should concern us: Motivation**
- ❖ **Where do irregularities come from: Low latitude/equatorial Electrodynamic**
- ❖ **Measurement Techniques for Irregularities in the Ionosphere**
- ❖ **Observations of Ionospheric Irregularities across the Africa sector**
- ❖ **Summary**
- ❖ **References**

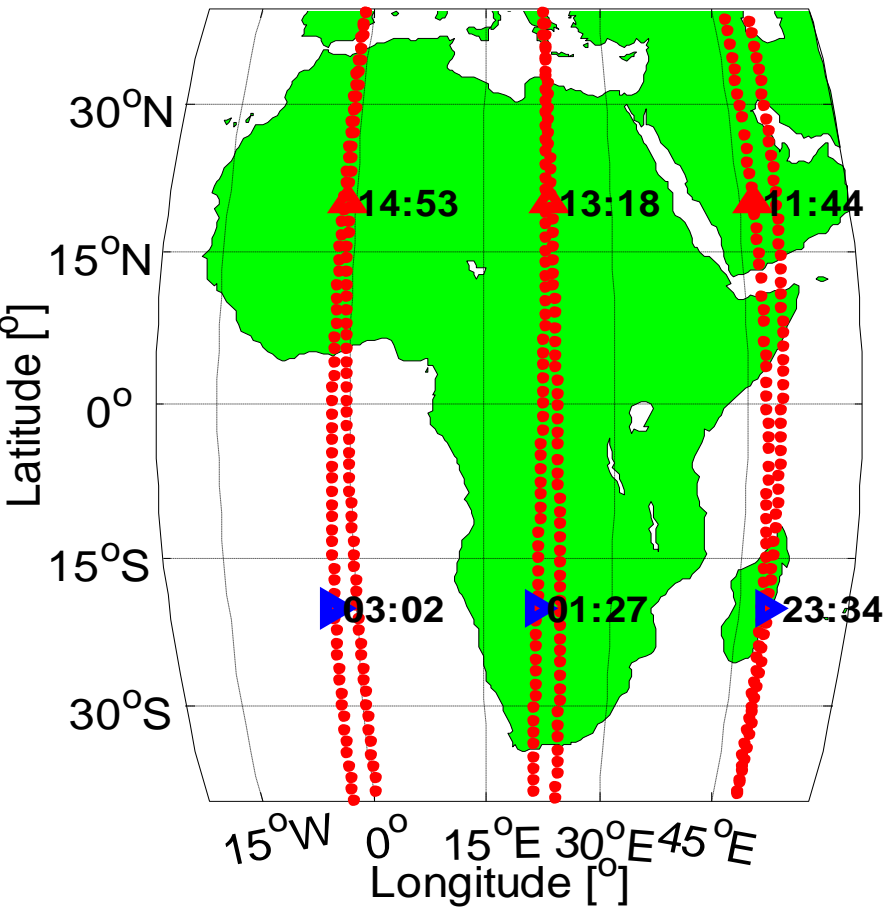
# Ionization levels from ground observations: Smooth vs. Irregular Ionosphere



The ionization throughout the day is smooth with VTEC variations arising from change in ionization levels based on solar zenith angle. After sunset VTEC irregularities appear due to EPBs causing fluctuations in ionization density.

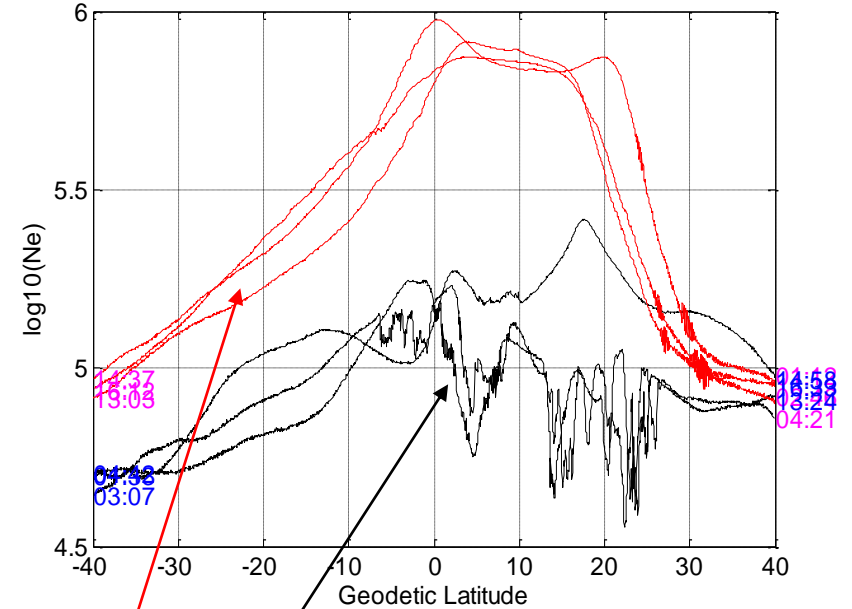
# Irregularities mainly dominant at night: Africa region from space observation

SWARM B: 2016-03-07

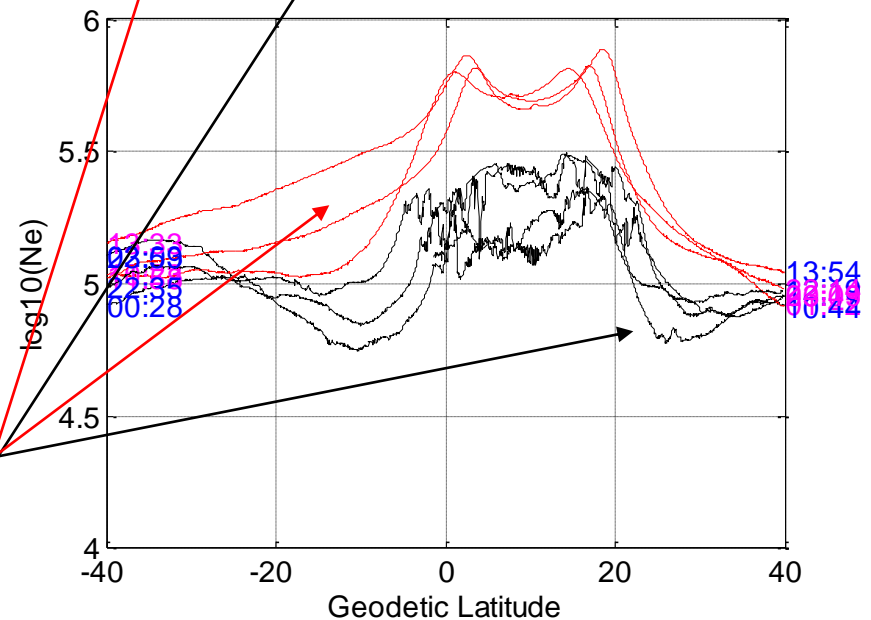


**Red lines** show day-time in-situ electron density measurements.  
**Black lines** are measurements during the post sunset hours.

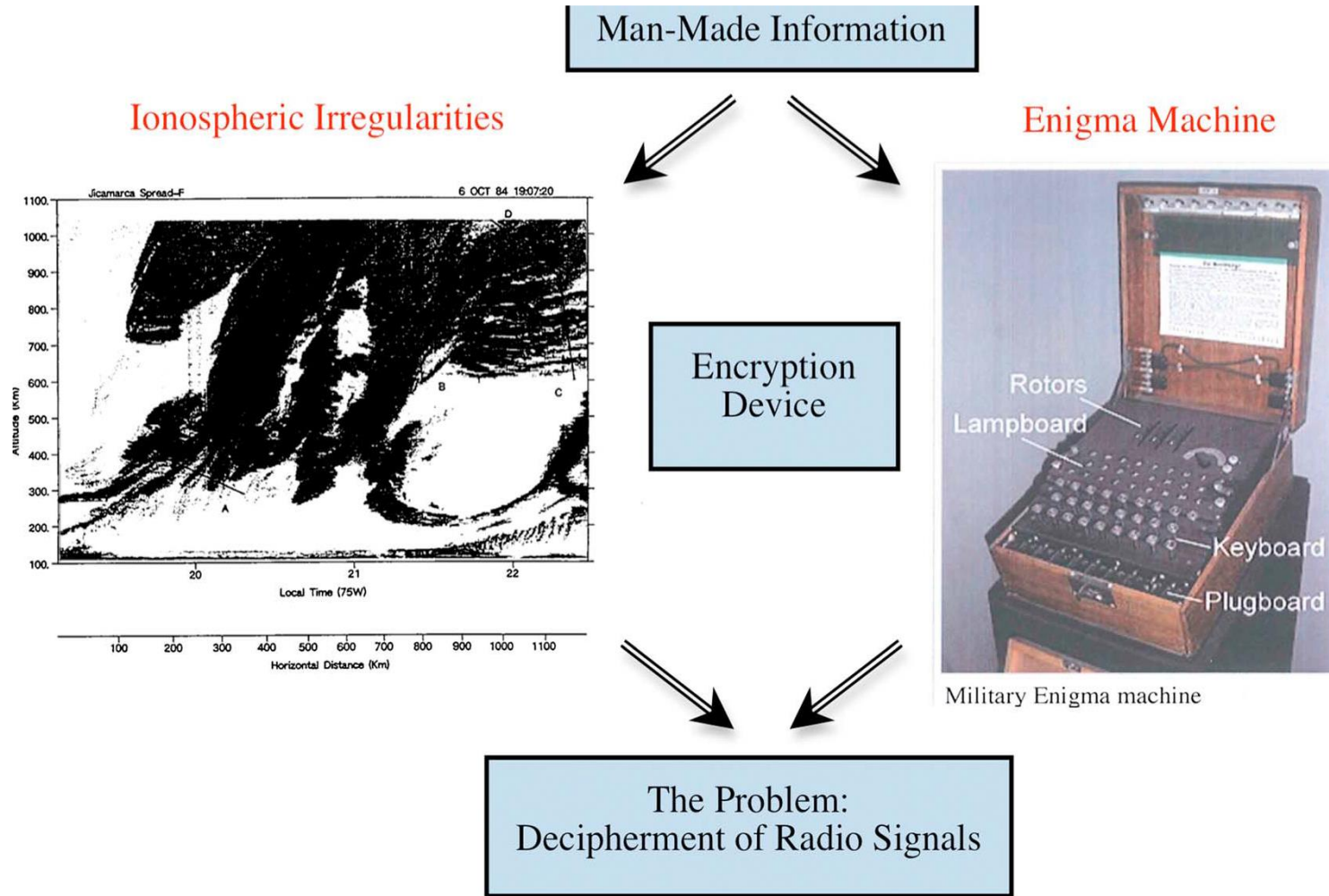
SWARM B Ne 07-Mar-2016



SWARM Ne 26-Mar-2016

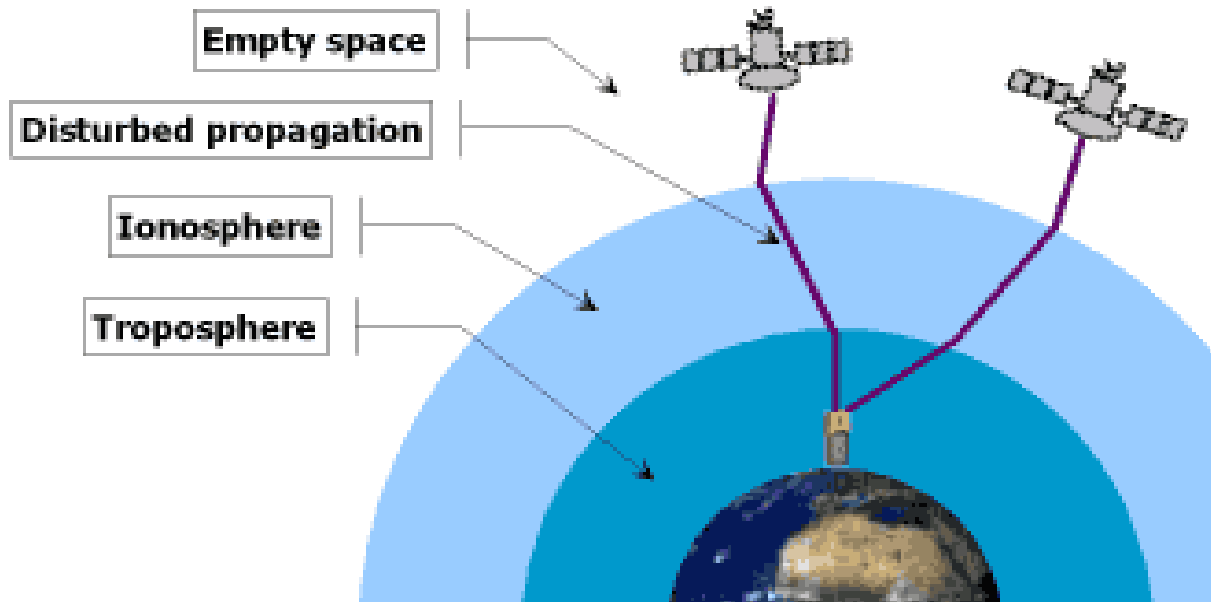


# Why should we be concerned about irregularities: Motivation 1 Impact on Technology and Human Activity (Economy):

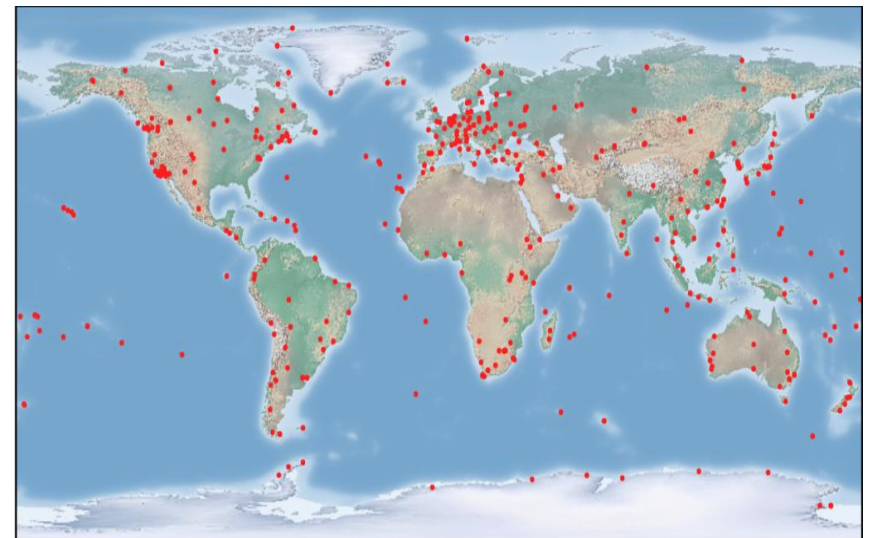


Courtesy: Jan Sojka SPACE WEATHER, VOL. 11, 134–137,  
doi:10.1002/swe.20041, 2013

# GNSS as a stand-alone research infrastructure: Motivation 2



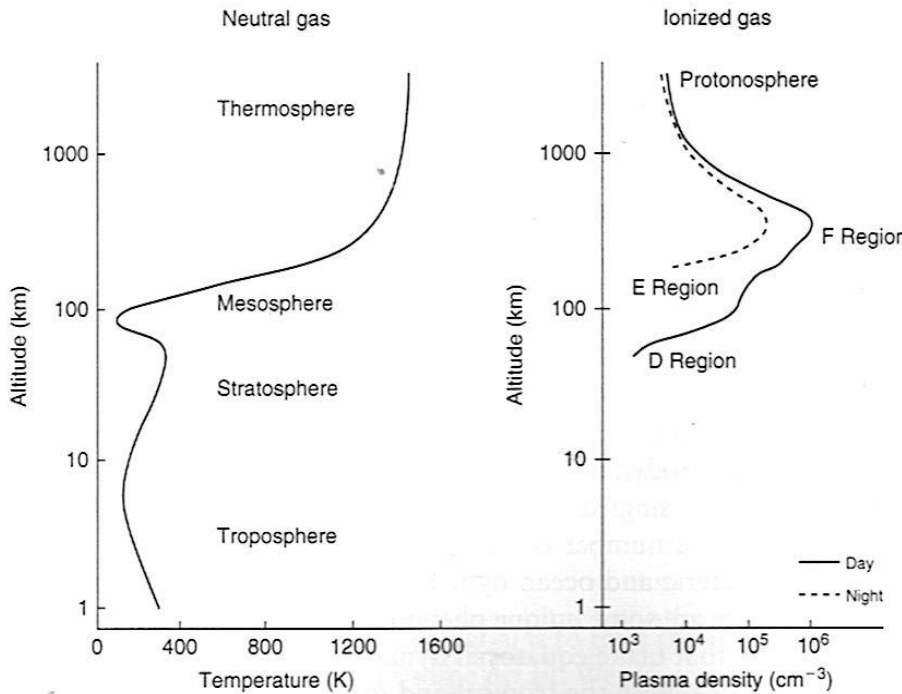
- **Seismic monitoring & prediction**
- **Volcano monitoring**
- **Climate change**
- **Gravity fields**
- **Atmospheric science**
  - ground water vapor
  - the ionosphere
  - space weather



IGS Stations, Last Updated 2019

Source: <https://www.igs.org/station-resources/>

# Where do irregularities come from in the low latitude ionosphere?



## plasma

- charged particles
- $n \approx n_i \approx n_e$

- Motion influenced by: g: gravity, p: pressure
- B : Magnetic field E : Electric field
- $v_{jn}$  : Collisions with neutrals

## Momentum Equation: Steady state

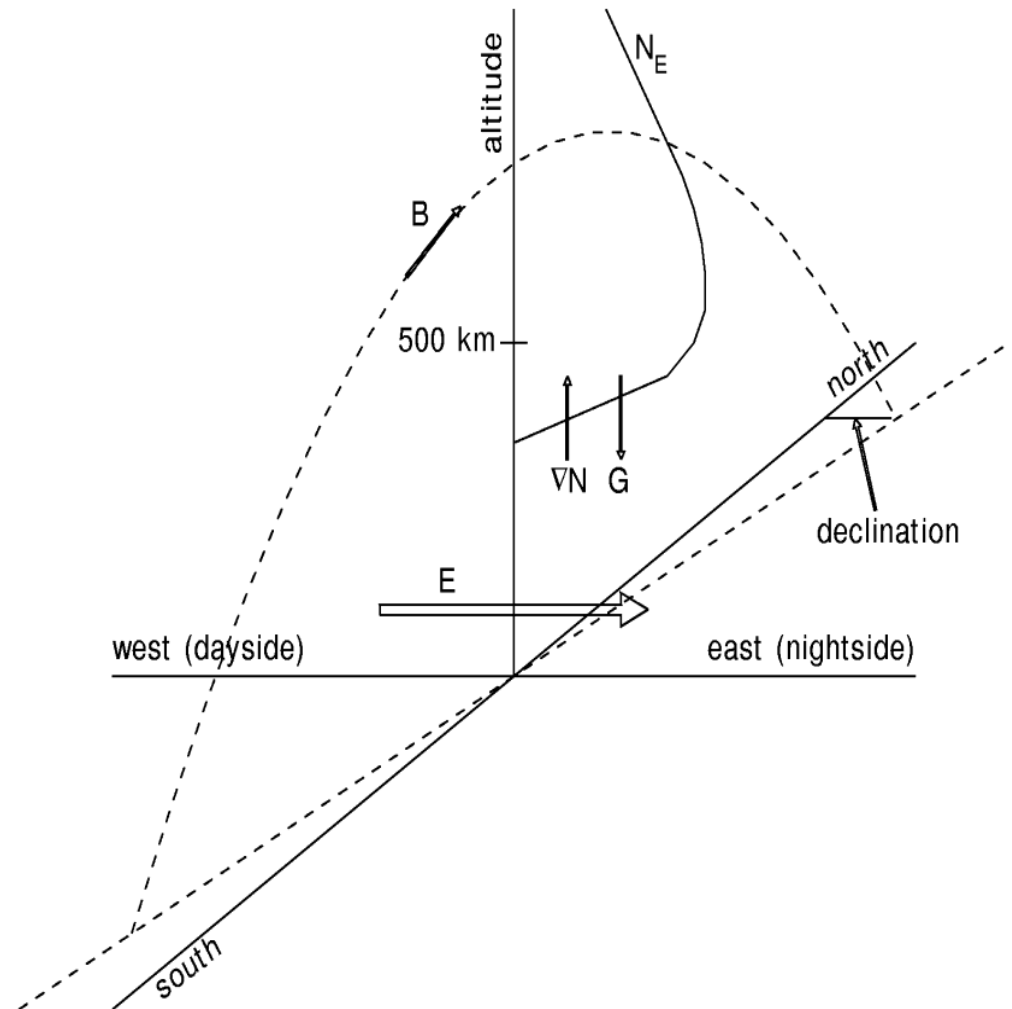
$$0 = -k_B T_j \nabla_j n + n M_j \vec{g} + ne(\vec{E} + \vec{V}_j \times \vec{B}) - n M_j \vec{v}_{jn} (\vec{V}_j - \vec{U})$$

Gravity points to  $n M_j \vec{g}$   
 Electric Field points to  $ne(\vec{E} + \vec{V}_j \times \vec{B})$   
 Pressure points to  $-k_B T_j \nabla_j n$   
 Magnetic Field points to  $\vec{V}_j \times \vec{B}$   
 Collision Freq with neutrals points to  $\vec{v}_{jn}$   
 Neutral wind velocity points to  $(\vec{V}_j - \vec{U})$

# Ionospheric dynamics at post-sunset hours

Towards dusk the enhanced zonal E is established to keep divergence  $J = 0$  from a sharp east-west (day-night) conductivity (density) gradient: Zonal E leads to pre-reversal enhancement in the eastward electric field.

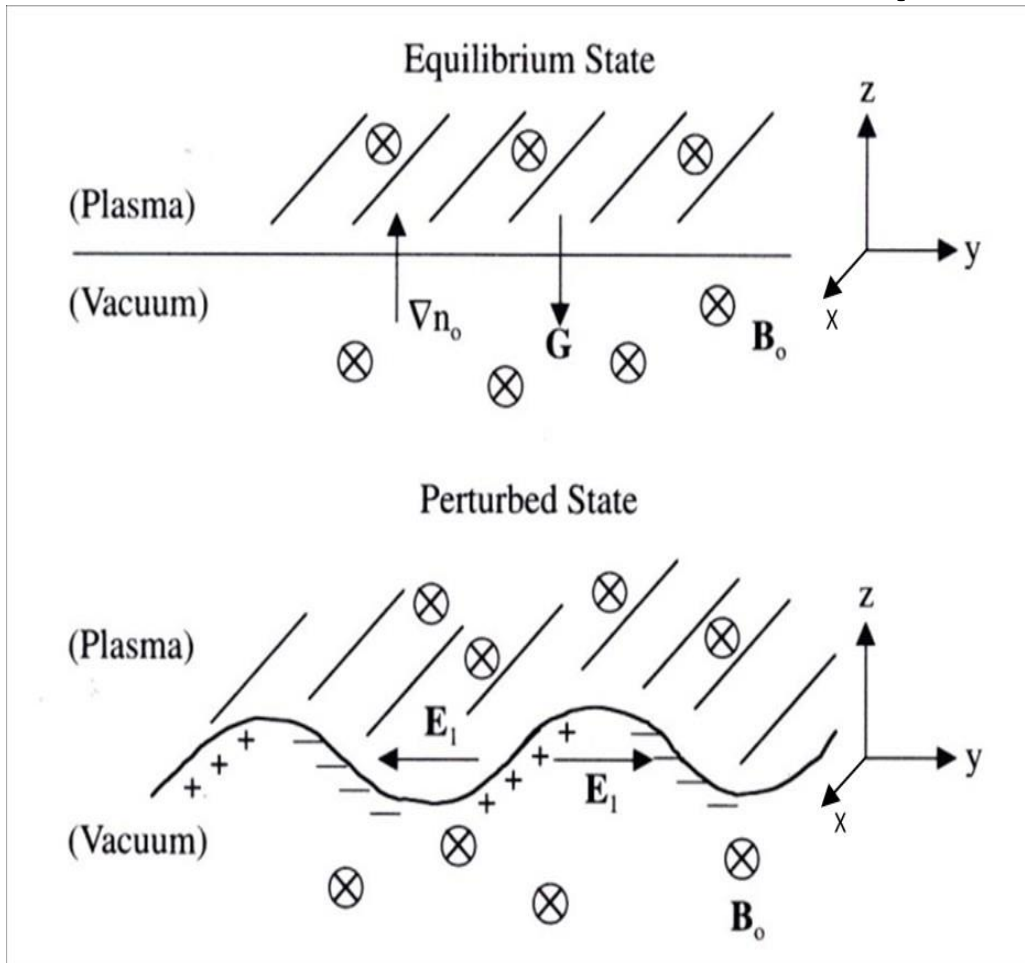
The F-layer thus rises as the ionosphere co-rotates into darkness. The ionization in the lower part rapidly decays and a steep vertical density gradient develops leading to a classical Rayleigh-Taylor (R-T) instability.



Schunk and Nagy, 2009, Figure 11.29



# Post Sunset Ionospheric Electrodynamics



Plasma instability: RT scenario

1. Sharp vertically upward gradient of plasma density.

2. Horizontal magnetic field lines

3. Currents driven by background electric fields

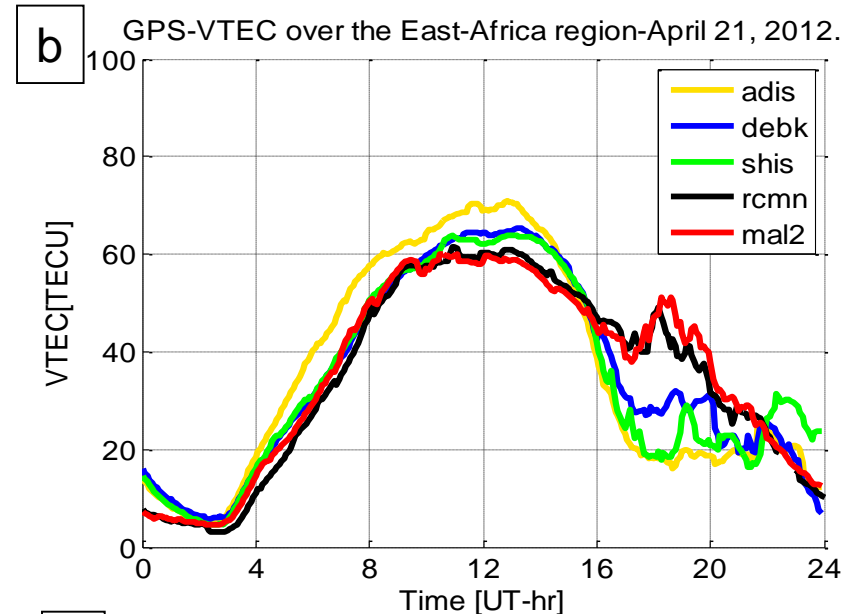
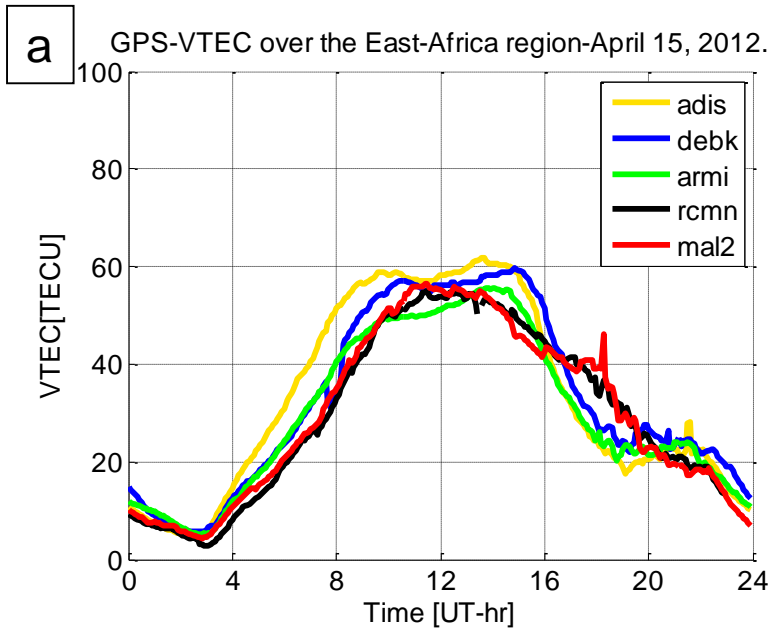
4. Gravity

Are all mutually perpendicular

[Schunk and Nagy, 2009, Figure 11.30]

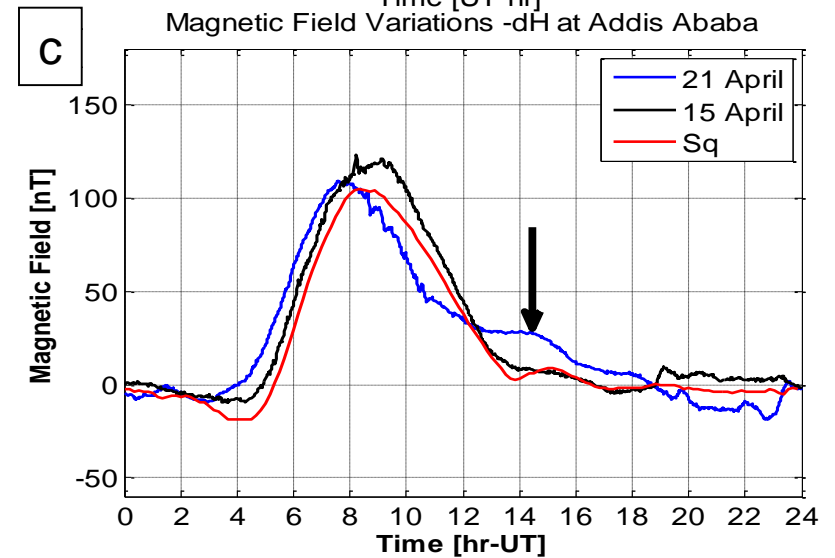
Bottom side unstable due to perturbation:  
density gradient against gravity.

# Observations of turbulent post sunset low latitude ionosphere:

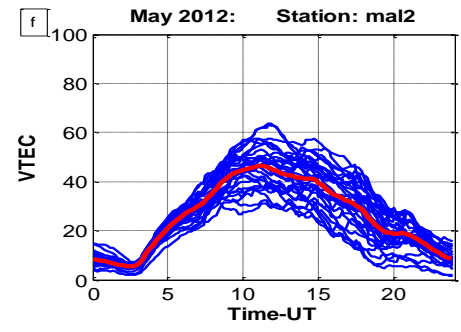
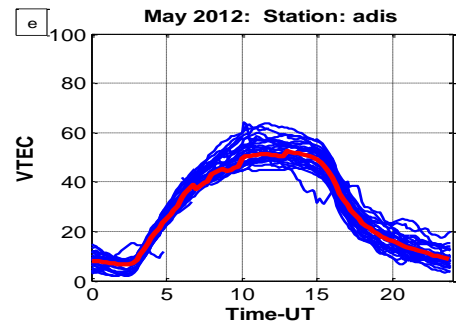
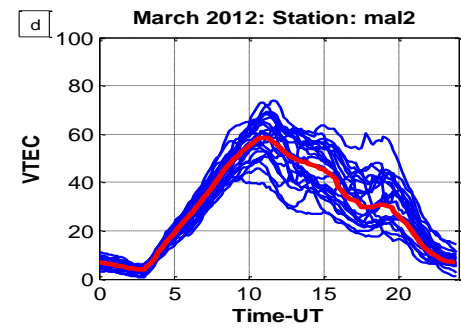
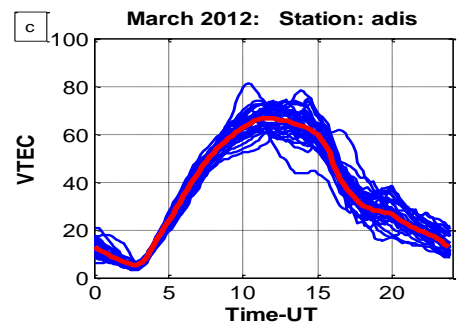
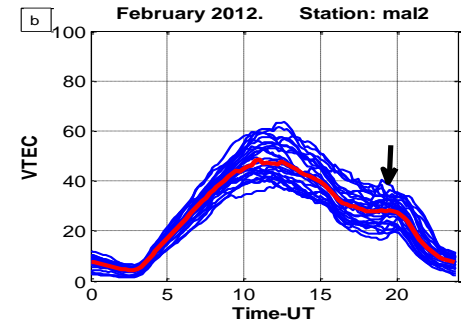
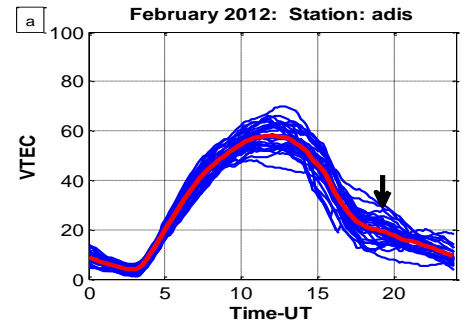
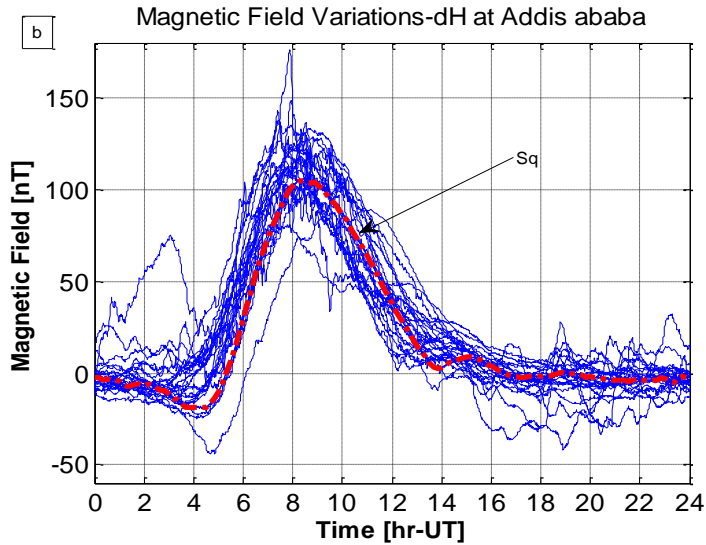


The **black** arrow shows an intense EEJ at sunset-local-PRE. This could be the cause of intense Post-sunset TEC enhancement on 21-April (Fig b)

*PRE= Prereversal Enhancement of Eastward electric field*



# How variable is the Post-sunset enhancement?



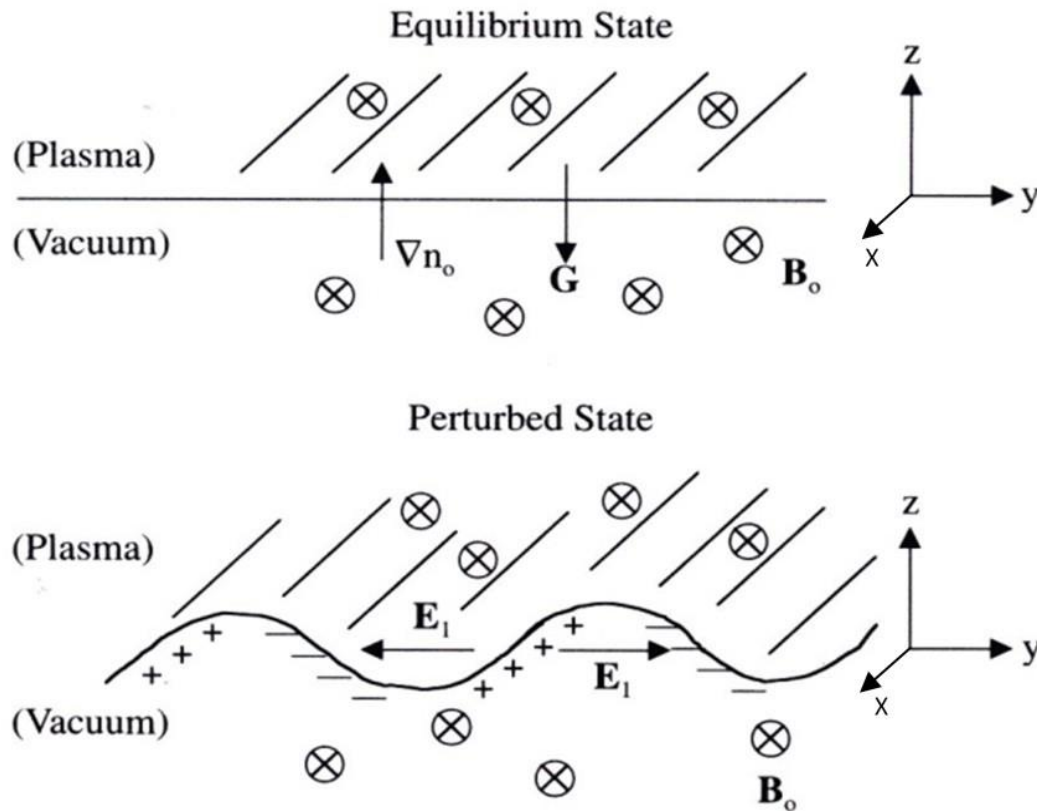
Post sunset enhancement is highly variable and depends on the magnitude of the PRE.

PRE cause plasma to be uplifted at the dip Equator. It then moves to the regions North and South of the dip equator and fluctuations in PRE leads to variability in TEC

Question? In the absence of PRE, do we still have the post-sunset TEC enhancement?

Depletions occurs at dip equator at sunset and enhances occur North and South of the dip equator.

# Where does the bottom side instability come from?



Plasma instability: RT scenario

1. Sharp vertically upward gradient of plasma density.
2. Pressure driven current does create not any perturbation electric fields
3. Pressure driven current flow parallel to the modulated density pattern and has no divergence.

[Schunk and Nagy, 2009, Figure 11.30

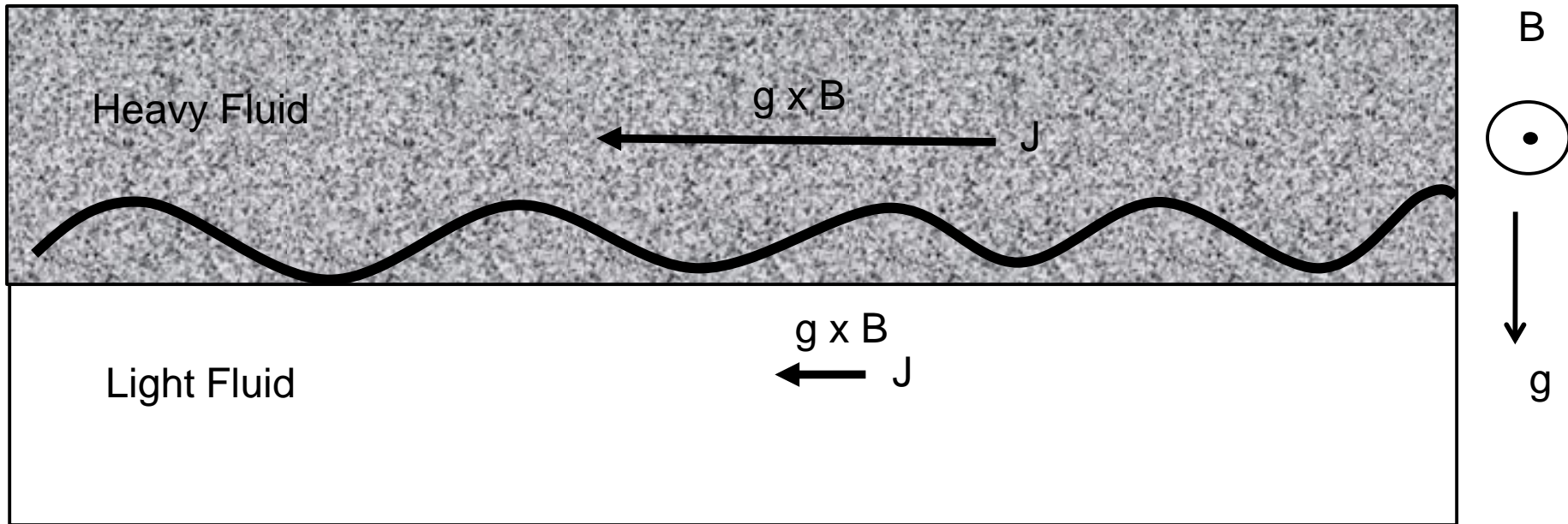
# Linear Theory of Rayleigh-Taylor Instability

Steady-state momentum eq.

$$0 = -k_B T_j \vec{\nabla} n + n M_j \vec{g} + ne(\vec{E} + \vec{V}_j \times \vec{B}) - n M_j v_{jn} (\vec{V}_j - \vec{U})$$

**J is proportional to density**

$$J = ne(V_i)_\perp = n M_i \vec{g} \times \frac{\vec{B}}{B^2}$$



# Linear Theory of Rayleigh-Taylor Instability

Steady-state momentum eq.

$$0 = -\underline{k_B T_j \vec{\nabla} n} + \boxed{n M_j \vec{g}} + ne(\vec{E} + \boxed{\vec{V}_j \times \vec{B}}) - n M_j \cancel{v_{jn}} (\vec{V}_j - \vec{U})$$

**J is proportional to electron density**       $J = ne(V_i)_\perp = n M_i \vec{g} \times \frac{\vec{B}}{B^2}$

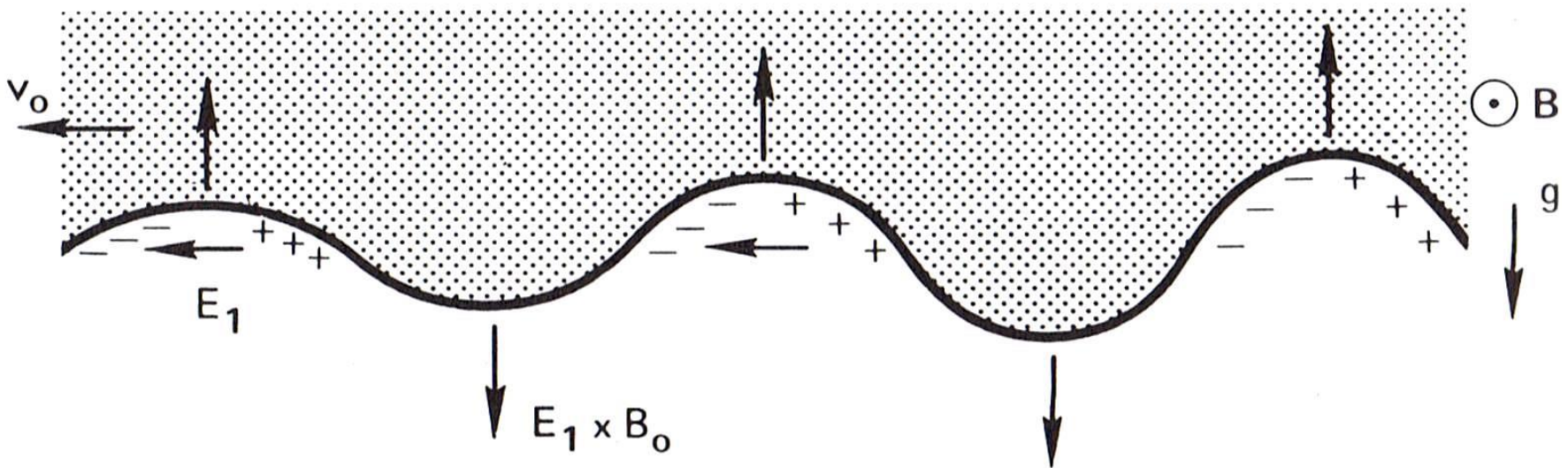
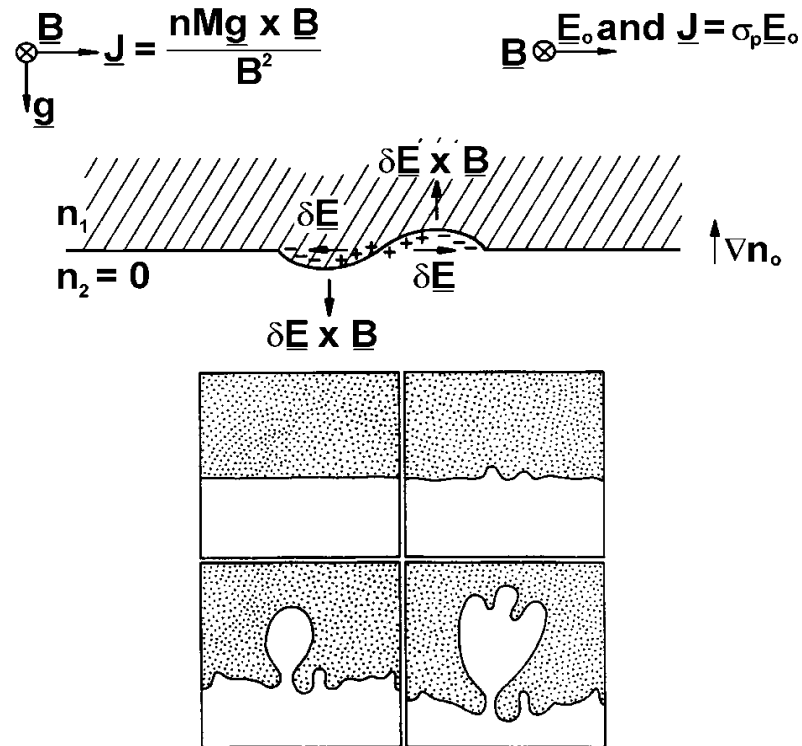


Image from F. F. Chen, Plasma Physics textbook

# Post Sunset Ionospheric Electrodynamics



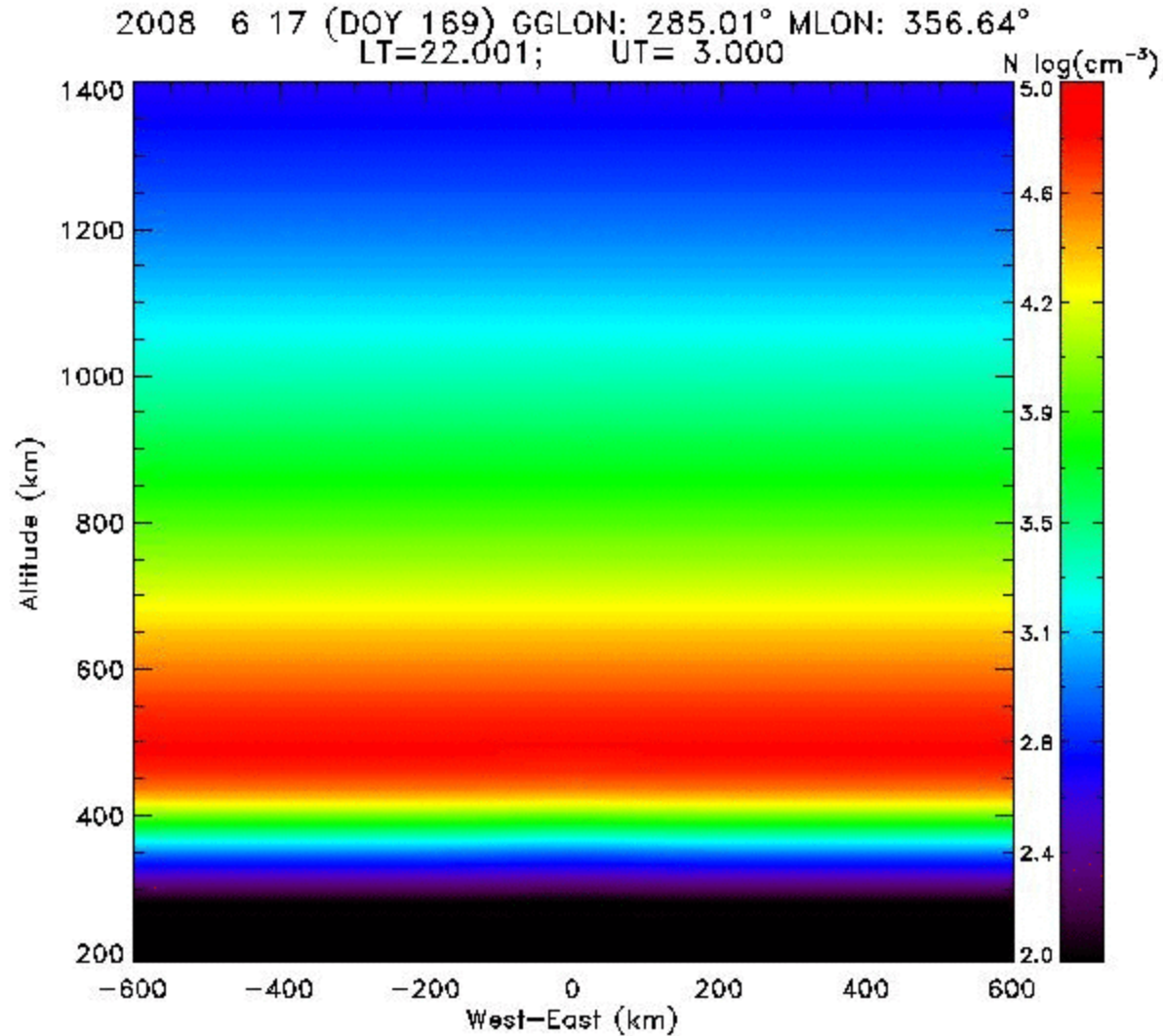
[Schunk and Nagy, 2009, Figure 11.30]

An exponential growth of instability

$$A = A_0 e^{\gamma t} \quad \gamma \approx \frac{\sum_F}{\sum_F + \sum_E} \left[ \frac{\mathbf{E} \times \mathbf{B}}{B^2} + U_n + \frac{g}{v^{eff}} \right] \frac{1}{N} \frac{\partial N}{\partial h}$$

# Nonlinear R-T Instability:

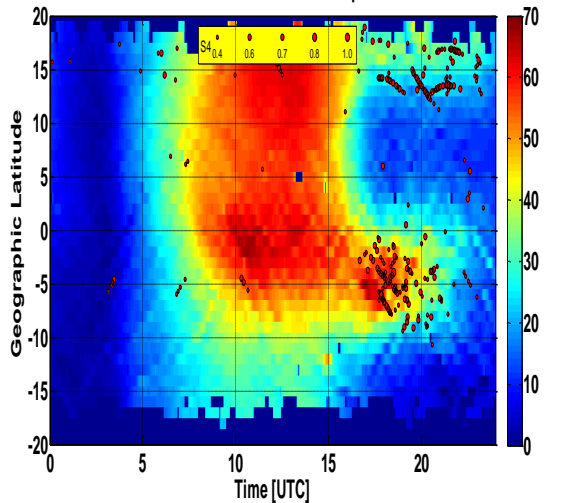
Credit: Prof Ron Caton of AFRL – PBMOD



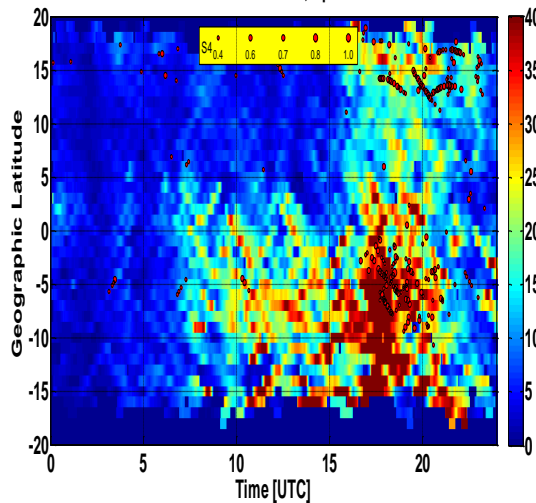


# Conditions Favorable for Irregularity Formation into multi-scale sizes

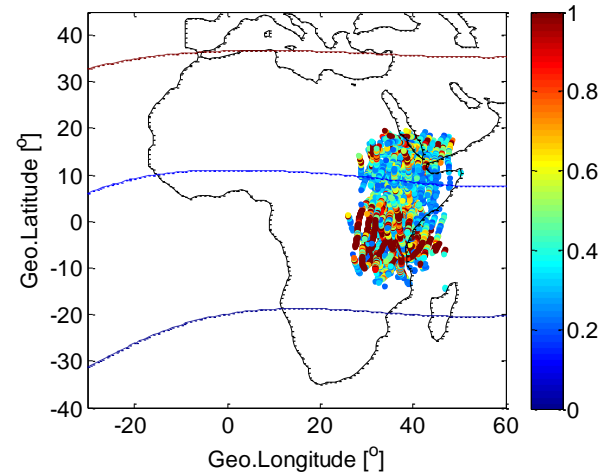
TEC for East Africa Sector 21 Apr 2012



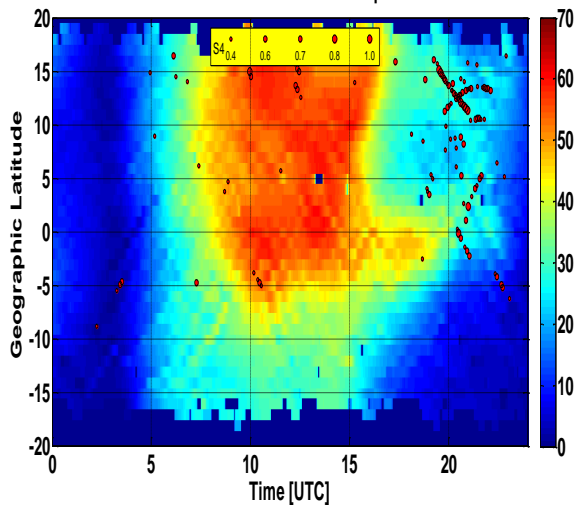
TEC Gradients: 21, Apr 2012



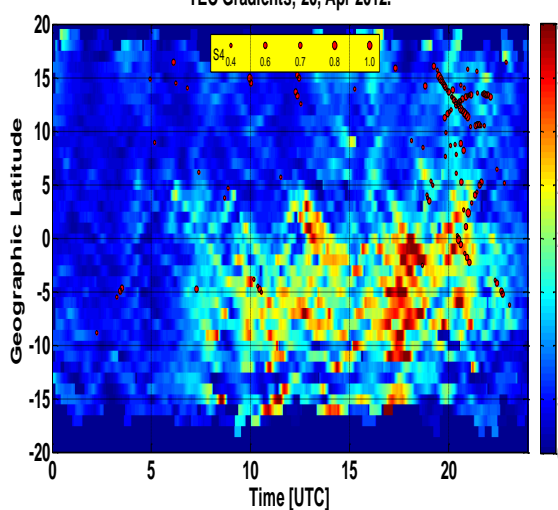
21, Apr 2012. Time: 17:00 - 23:00UT



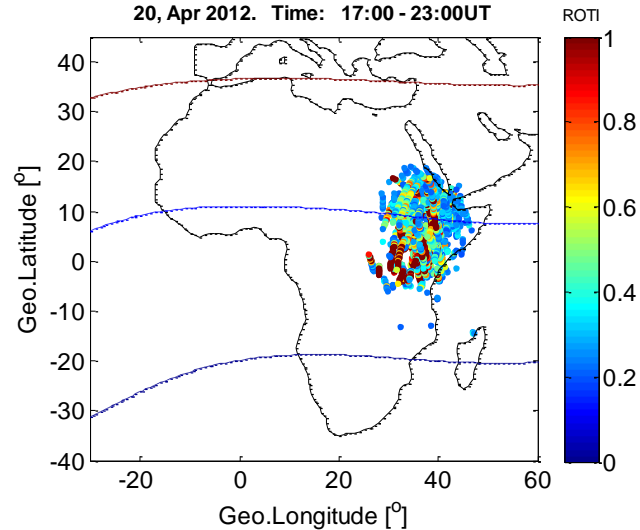
TEC for East Africa Sector 20 Apr 2012



TEC Gradients; 20, Apr 2012.



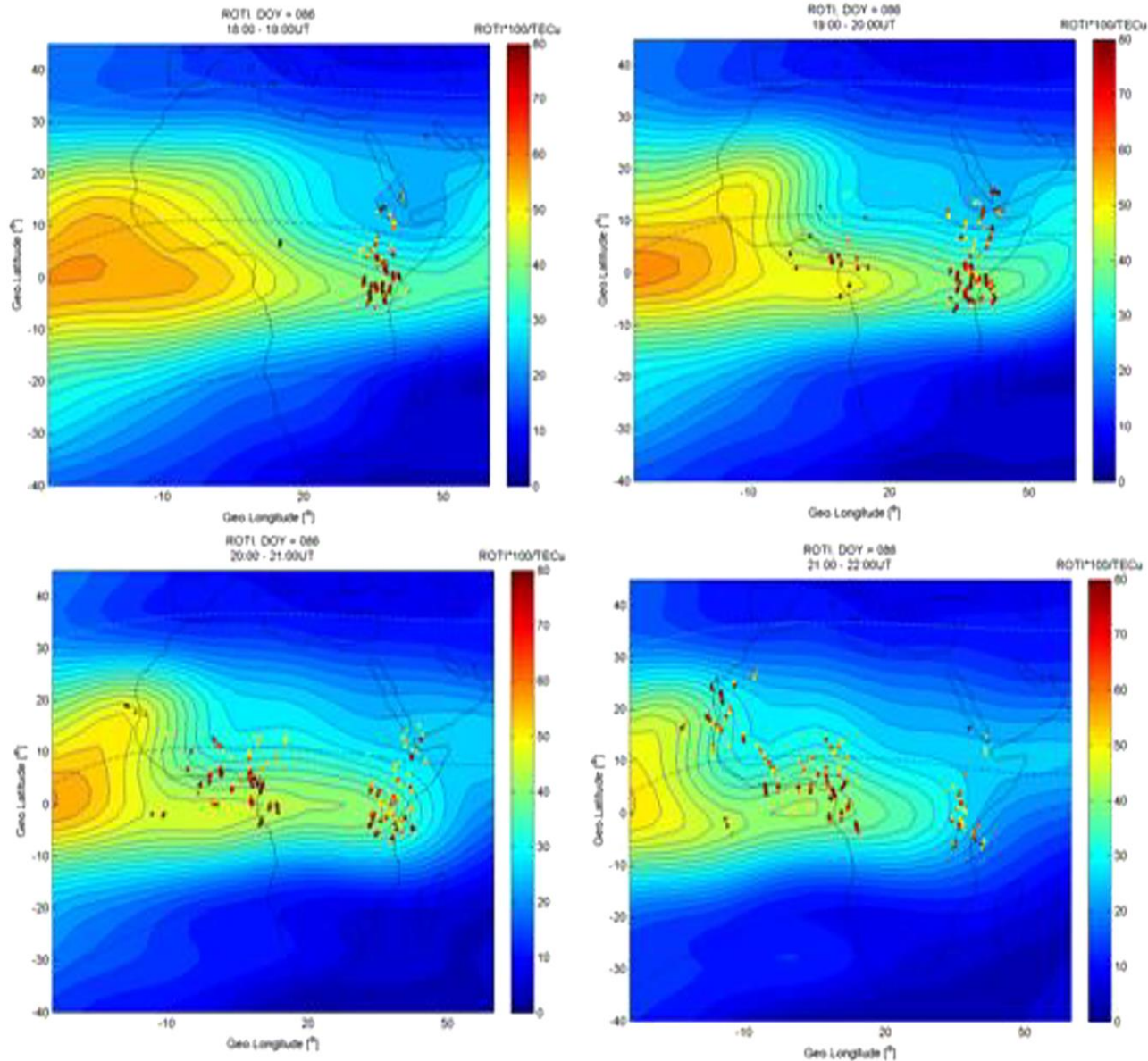
20, Apr 2012. Time: 17:00 - 23:00UT



# Conditions Favorable for Irregularity Formation into multi-scale sizes

GIM for 26 Mar 2016.

Time from 18: UT to 21 UT

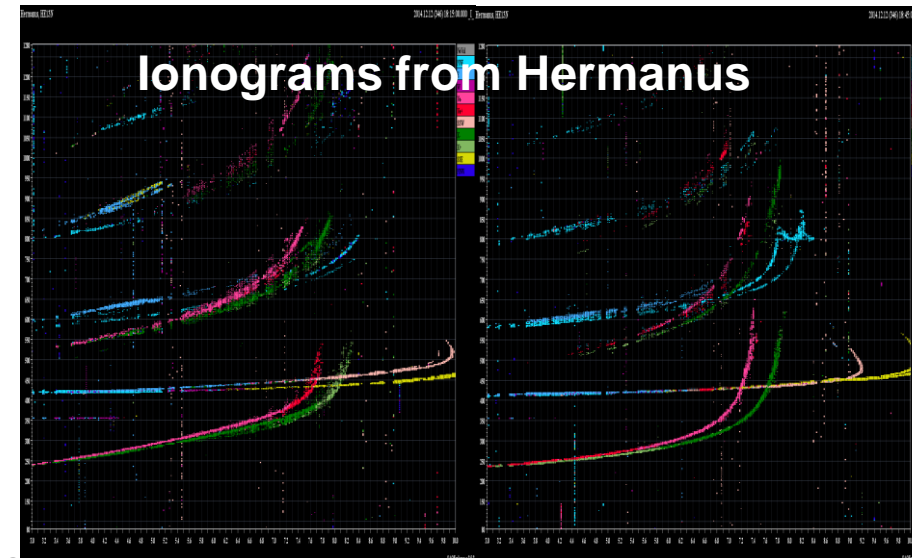
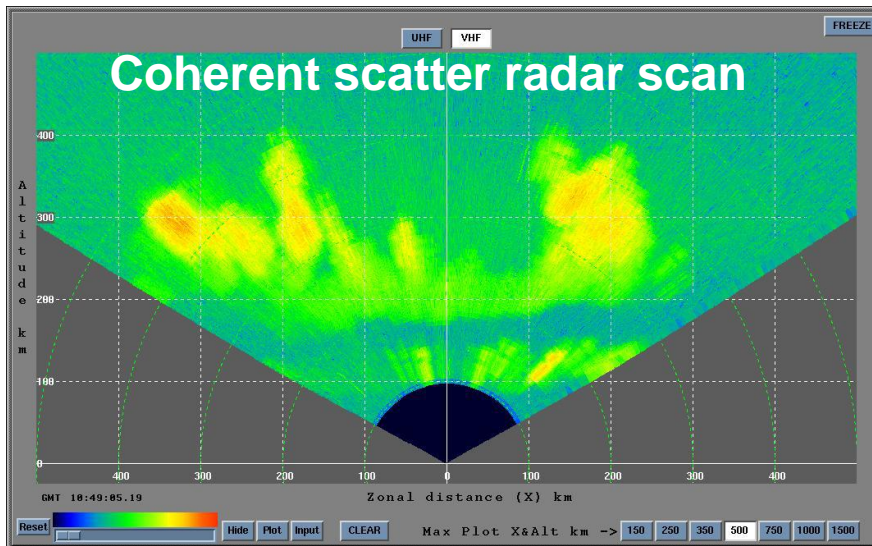
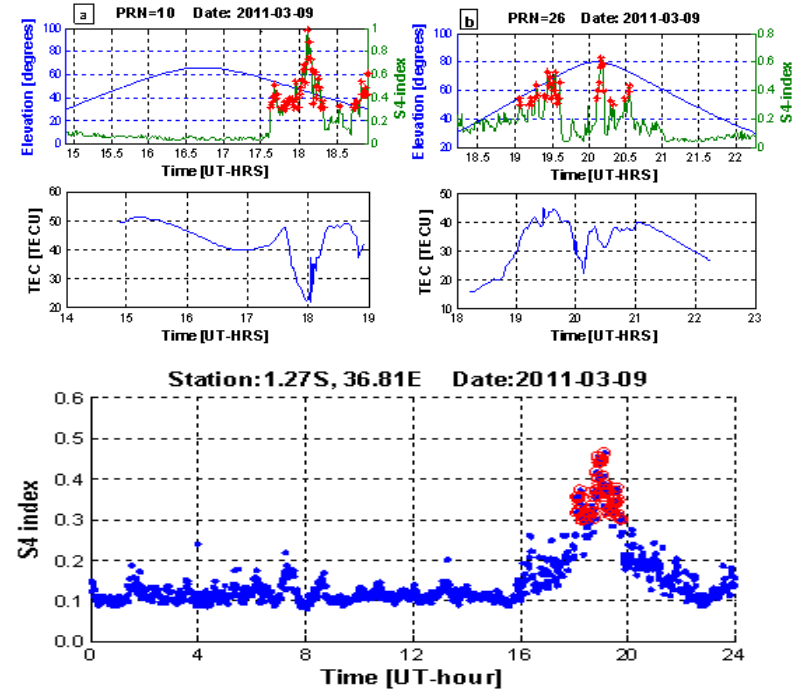


**Question to participants:**

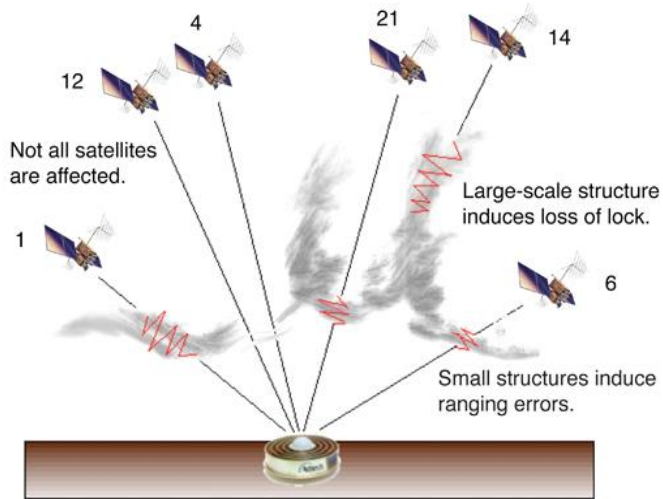
**Why don't we have ionospheric irregularities forming during Daytime?**

# How do we detect the irregularities/plasma depletions ?

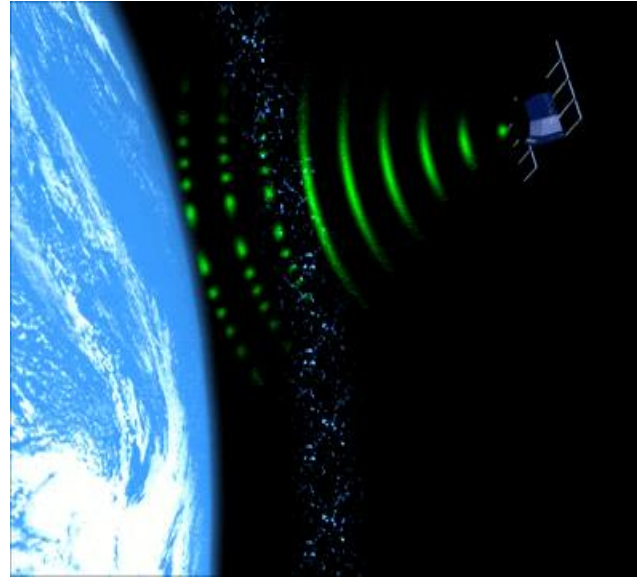
- Coherent and incoherent scatter radar.
- In-situ satellite-borne space probe
- Radio occultation and scintillation measurement
- Airglow detectors
- Ionosondes



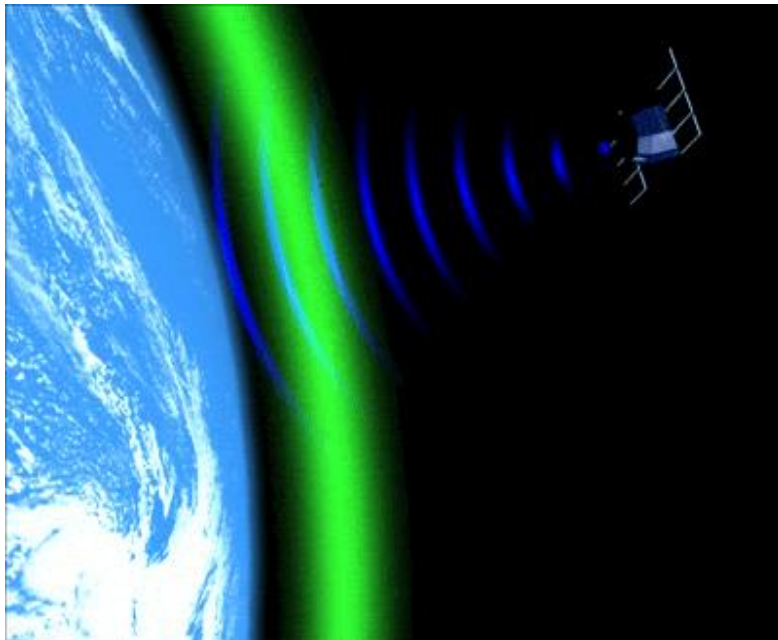
# Research Techniques and methodology:



Courtesy: GPS World



Courtesy:  
Bath University



Amplitude  
Scintillation

$$S_4 = \sqrt{\frac{\langle I^2 \rangle - \langle I \rangle^2}{\langle I \rangle^2}}$$

$$ROT = \frac{TEC_k^i - TEC_{k-1}^i}{t_k - t_{k-1}}$$

$$ROTI = \sqrt{\langle ROT^2 \rangle - \langle ROT \rangle^2}$$

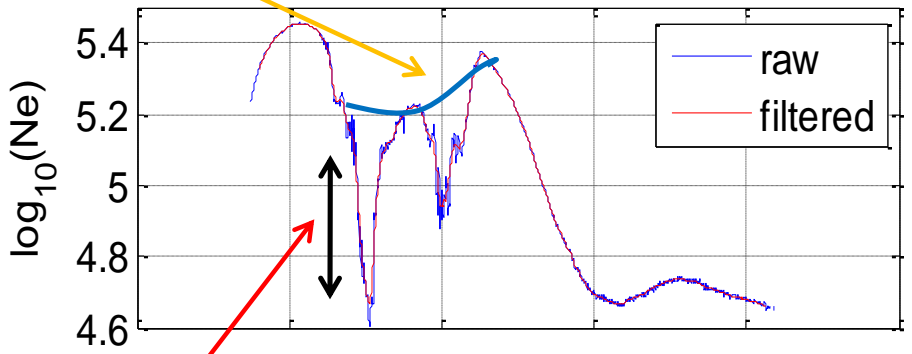
# Irregularity Activity based on in-situ electron density variations measured by LEO Satellites e.g. Swarm, CHAMP

1. Irregularity activity:  $\frac{\Delta N}{N}$  Dao et al., 2011

$\Delta N$  = difference in electron density from the ambient density

$N$ - ambient density: the envelope connecting the total maxima of electron density measure evaluated at a given time with a spline interpolation

SWARM Ne 20-Mar-2016, mean longitude 44.20 °



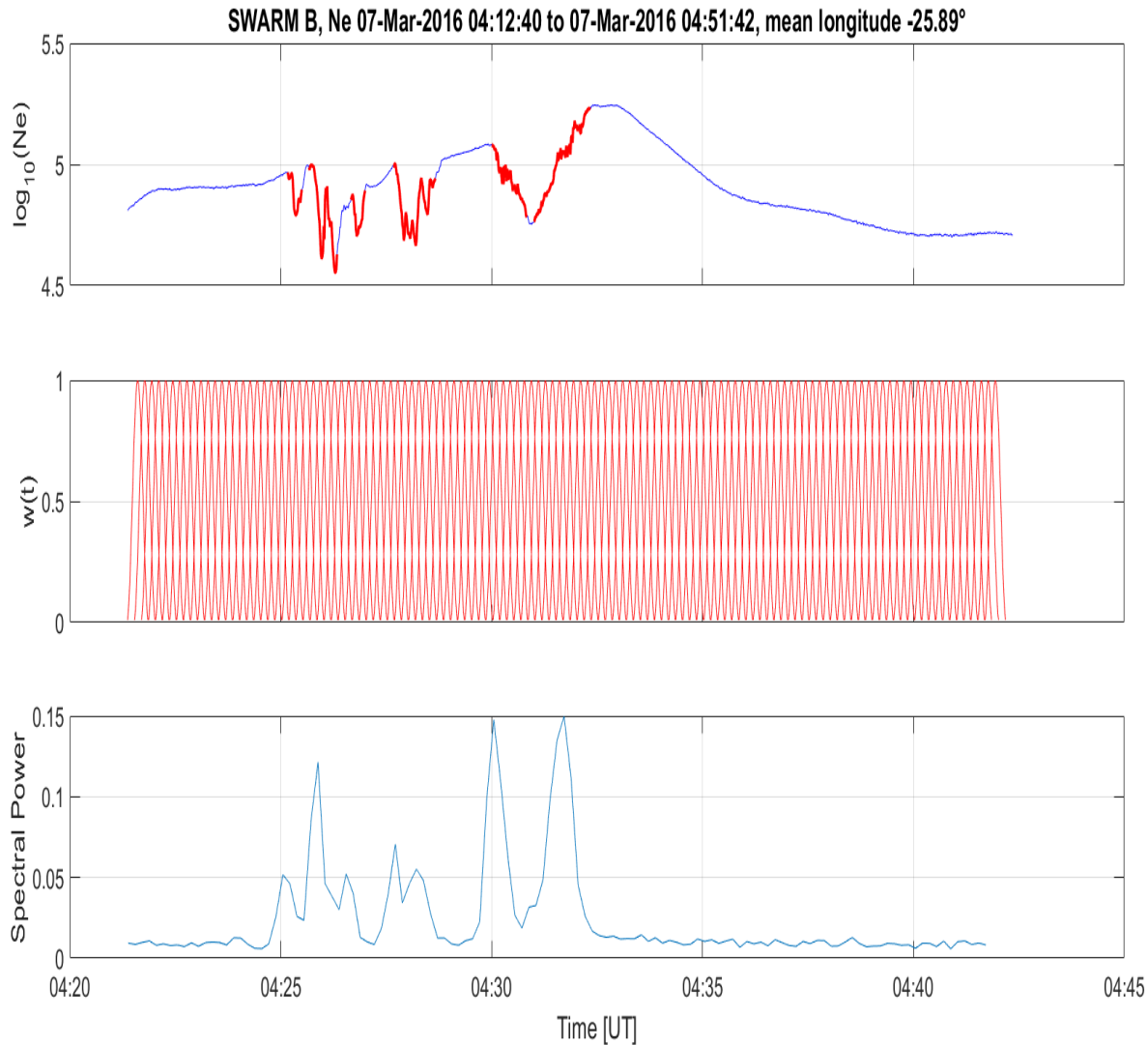
Delta N

$$RODI = \sqrt{\langle ROD^2 \rangle - \langle ROD \rangle^2}$$

$ROD = d(N_e)/dt$  is the rate of change of the detrended in-situ electron density.

**RODI was first mentioned by Zhakharenkova et al., (2016) and compared it to ROTI derived from GPS receiver onboard CHAMP**

# Ne spectral power



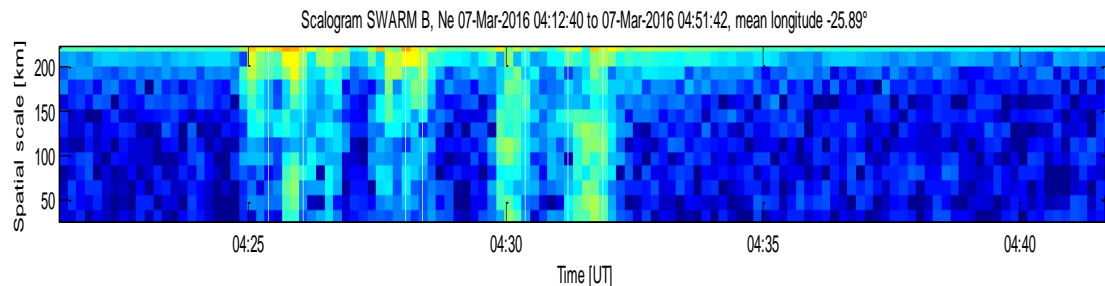
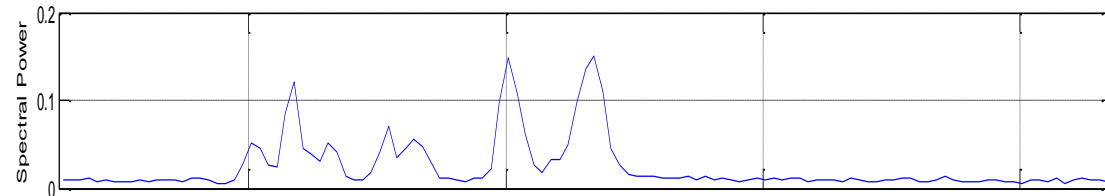
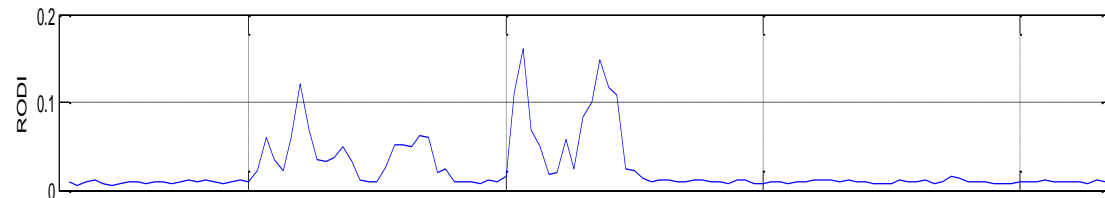
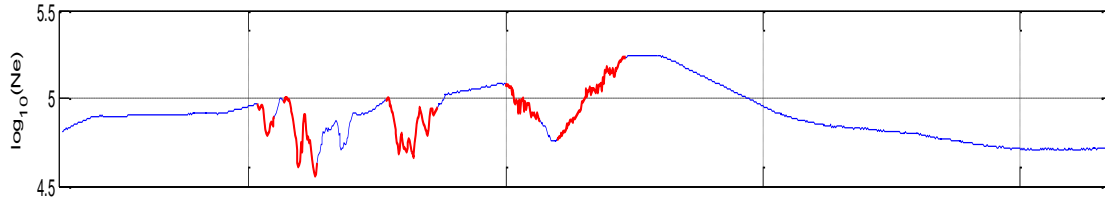
Red lines show extent of structures

$w(t)$  plot show the Hanning windows used for the STFT. The windows are spaced 10 seconds apart and are 30 seconds wide

Spectral power -total energy in the frequency range 0.15 Hz to 0.5 Hz at each 10 s interval.

# Multi-scale structures seen in-situ electron density

SWARM B, Ne 07-Mar-2016 04:12:40 to 07-Mar-2016 04:51:42, mean longitude -25.89°



✓RODI closely follows the Spectral power, which allows us to infer that the RODI is indicative of the high-frequency fluctuations in the frequency band 0.15 Hz to 0.5 Hz.

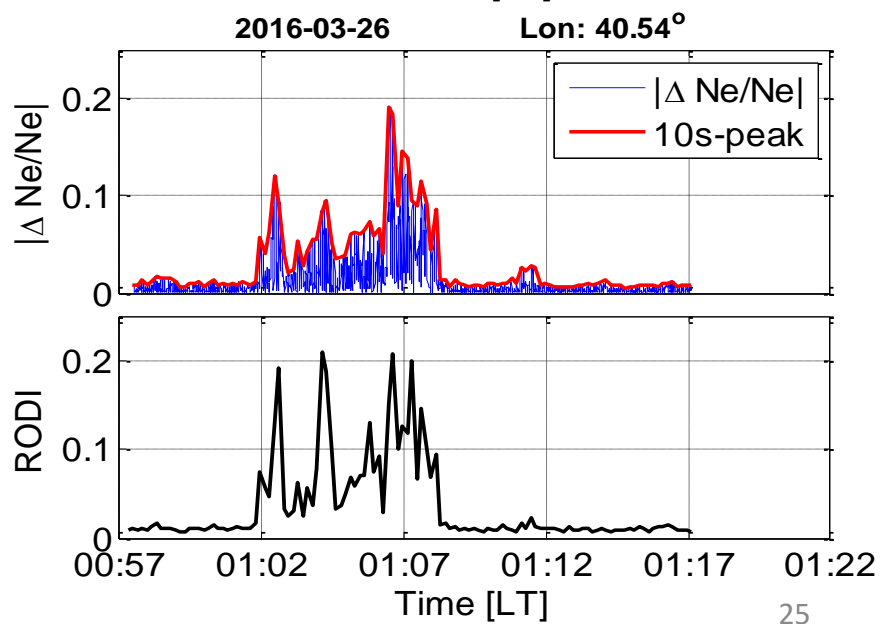
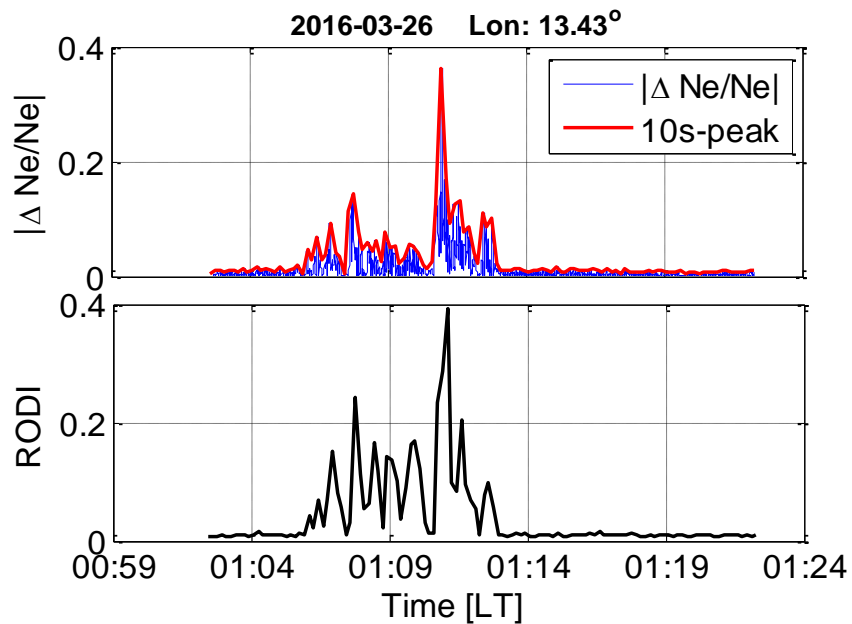
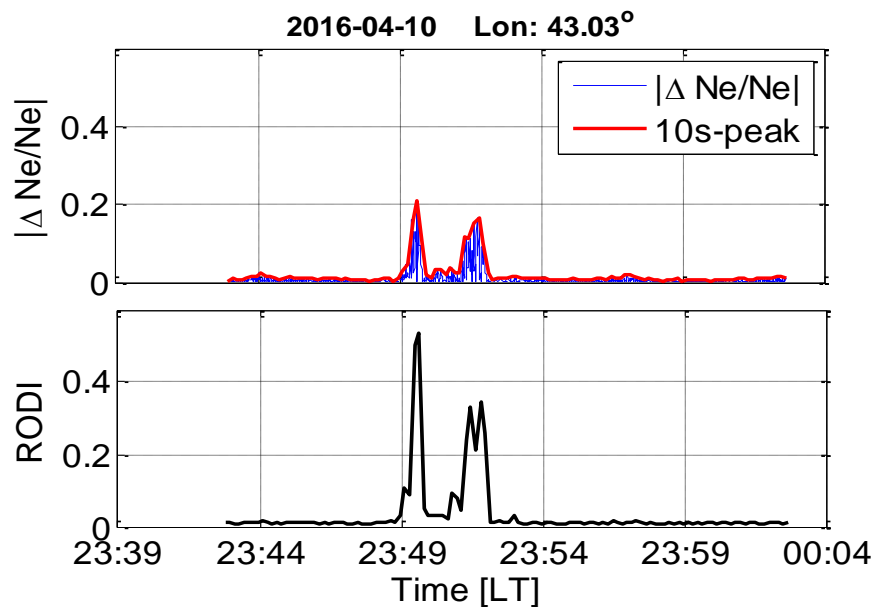
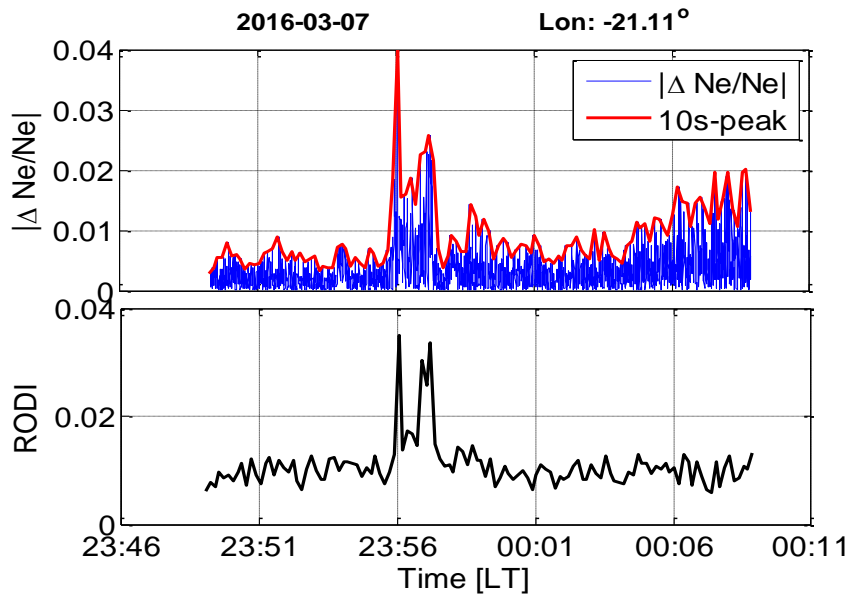
## Periodograms to Scalogram

Period=1/frequency

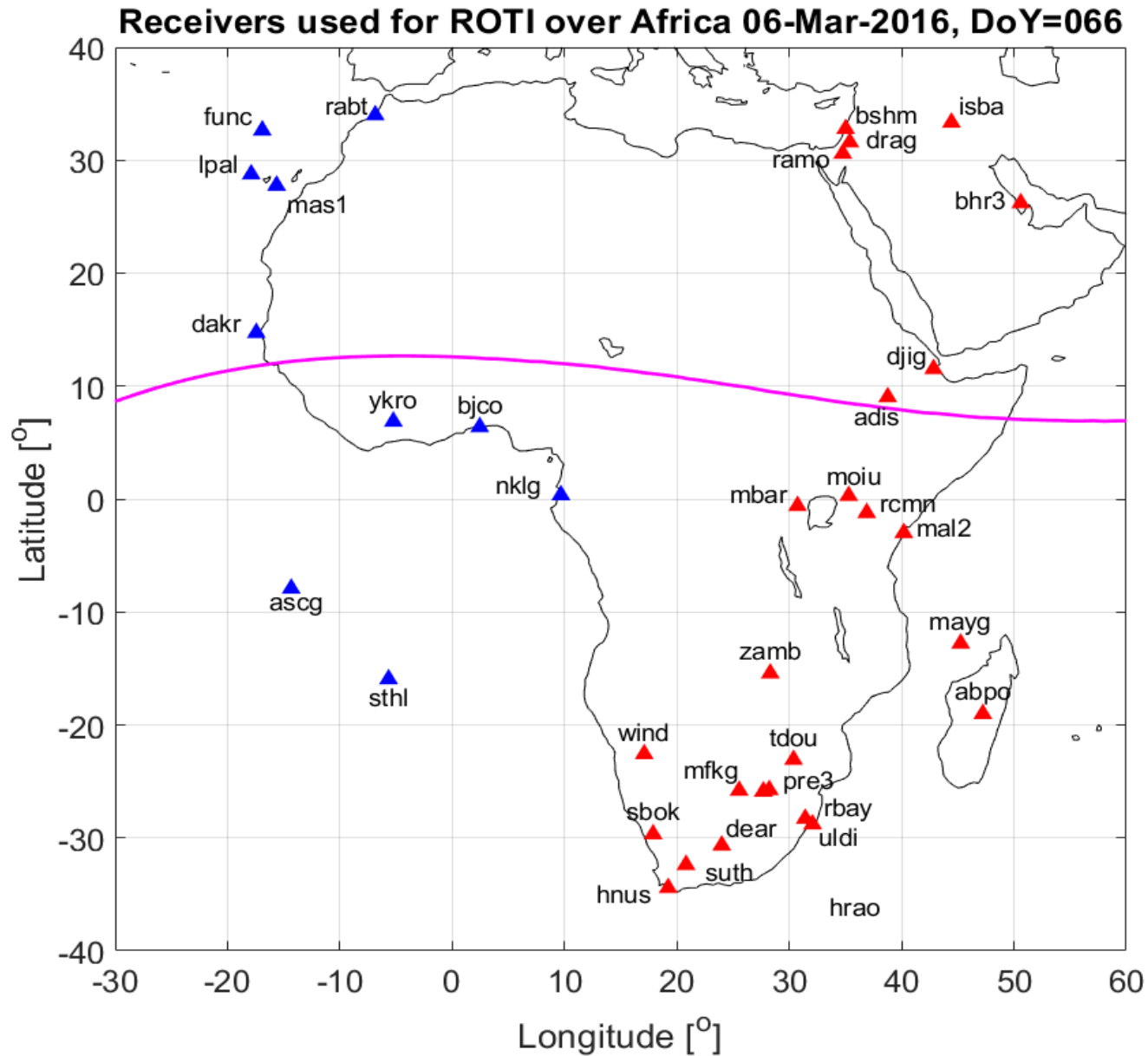
Scale = period \* orbit velocity



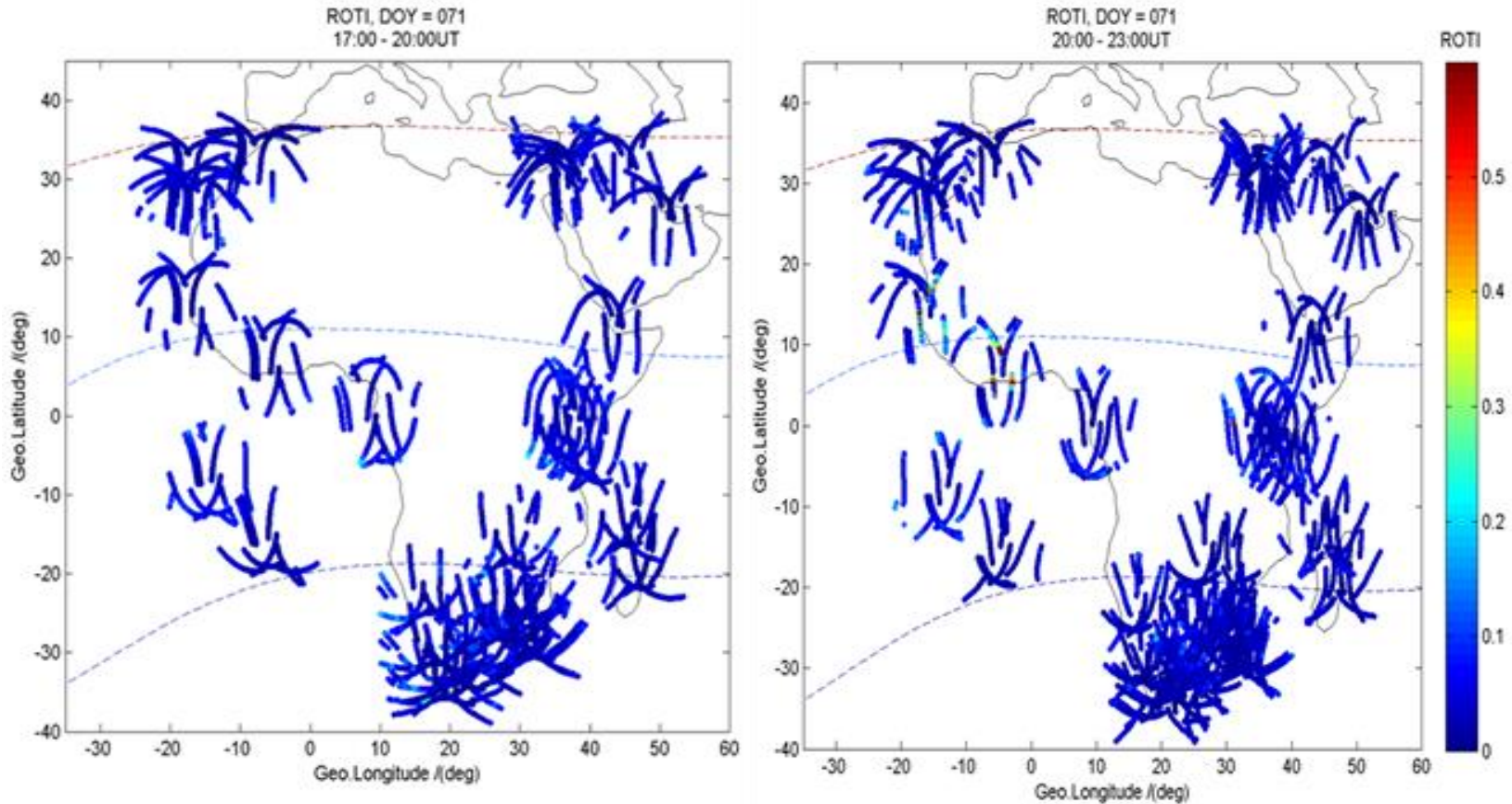
# Comparison of RODI to Delta N which also measures irregularity activity



# Irregularities across the African Sector: IGS Network Stations

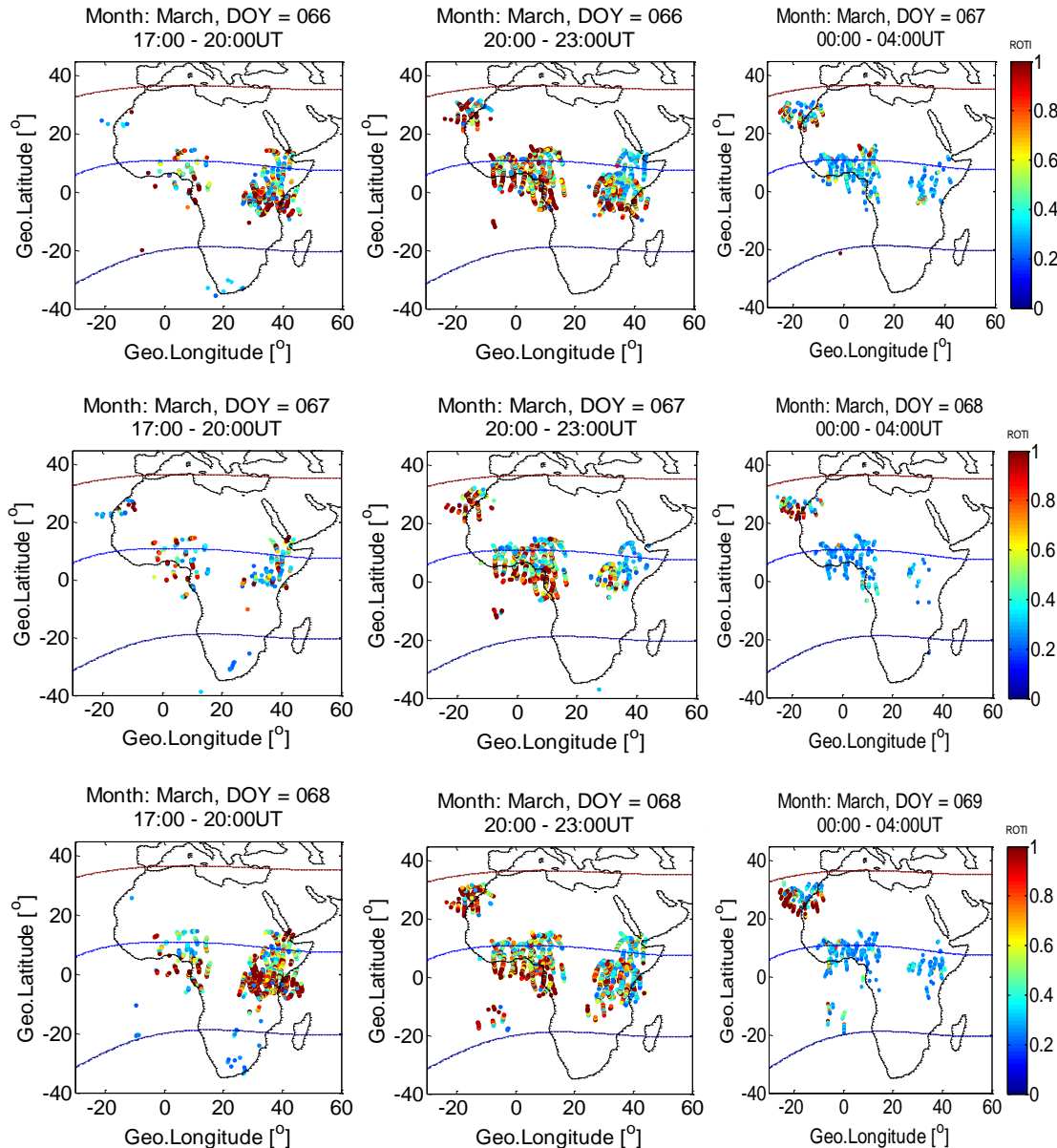


# Diurnal variation in irregularities across Africa



**Quiet-time observations of Rate of Total Electron Content Index (ROTI) in the range [0 0.6] for 11 March 2016 (day 71) during the periods 17:00-20:00 UT (left) and 20:00 to 23:00 UT (right). These maps over two 3-hour periods effectively depict the coverage by the available GNSS receivers.**

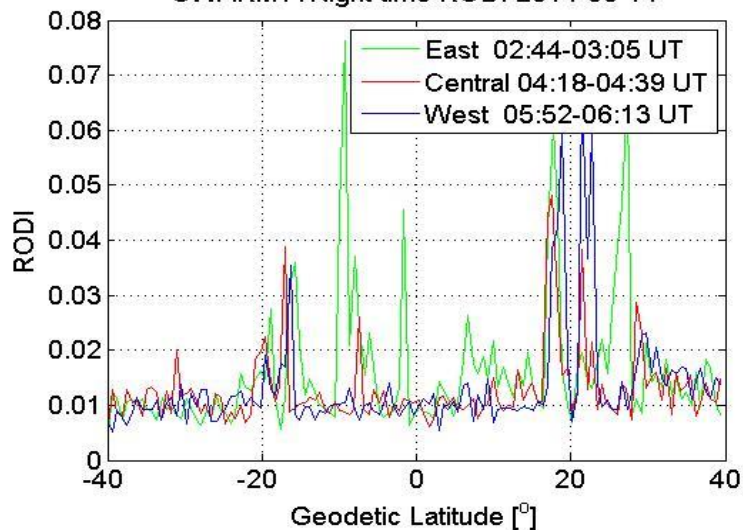
# Daily variation of Irregularities: Year of observation-2014



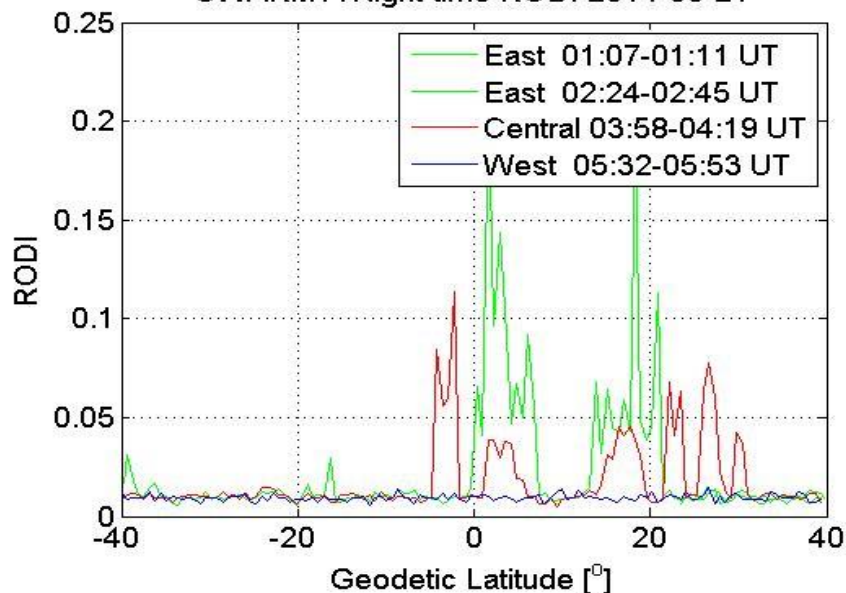
Temporal and spatial distribution of ionospheric irregularities (ROTI>0.2) across the African region during 7 to 9 March 2014 (days 66 to 68). ,

# Using LEO to fill the gaps in data coverage Across Africa: e.g. Swarms, CHAMP

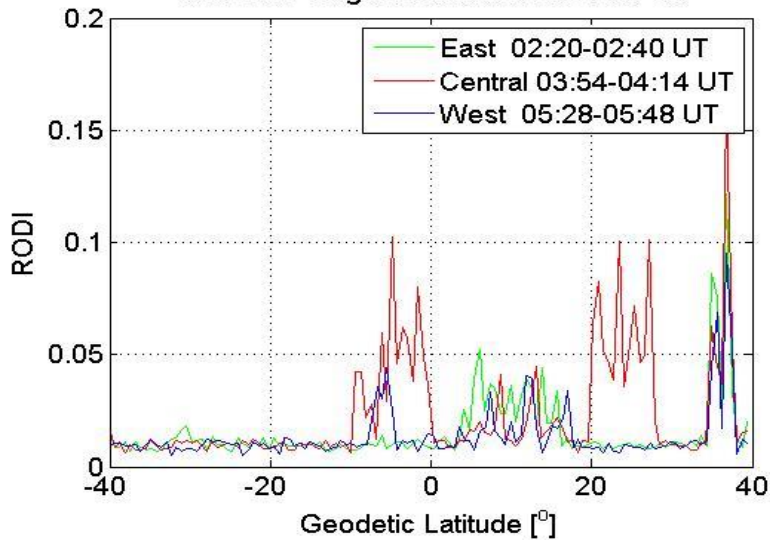
SWARM A Night-time RODI 2014-03-14



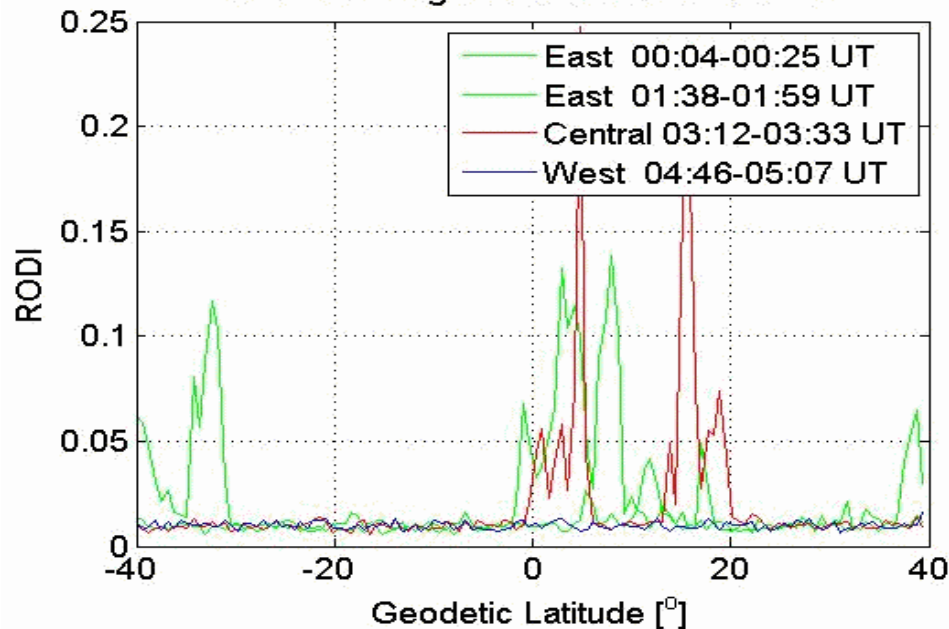
SWARM A Night-time RODI 2014-03-21



SWARM A Night-time RODI 2014-03-18

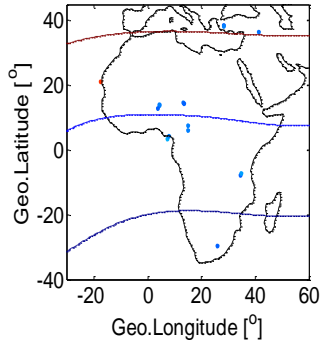


SWARM A Night-time RODI 2014-04-01

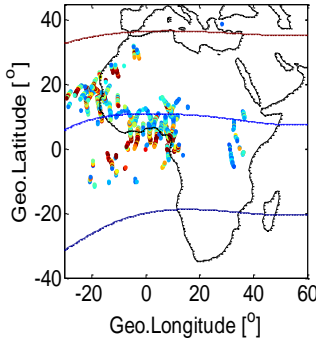


# Salient Features: Year of study 2016. Data Source: IGS network

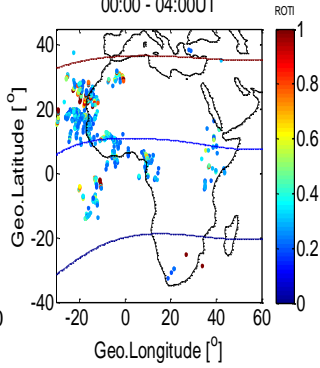
Month: March, DOY = 076  
17:00 - 20:00UT



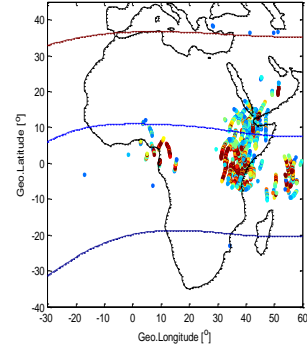
Month: March, DOY = 076  
20:00 - 23:00UT



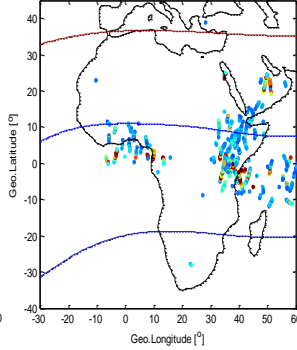
Month: March, DOY = 077  
00:00 - 04:00UT



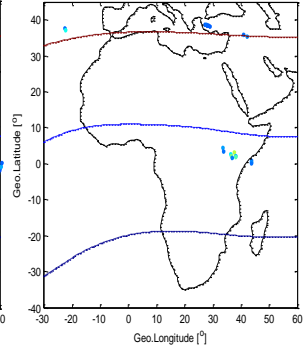
Month: March, DOY = 080  
17:00 - 20:00UT



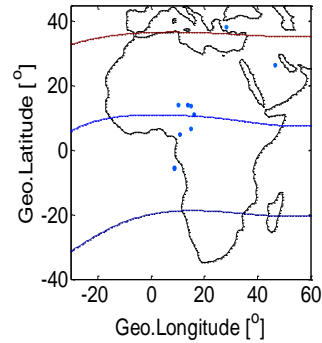
Month: March, DOY = 080  
20:00 - 23:00UT



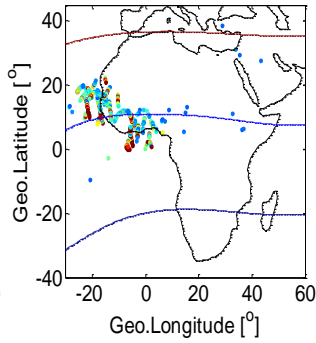
Month: March, DOY = 081  
00:00 - 04:00UT



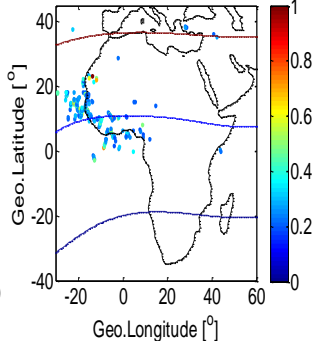
Month: March, DOY = 081  
17:00 - 20:00UT



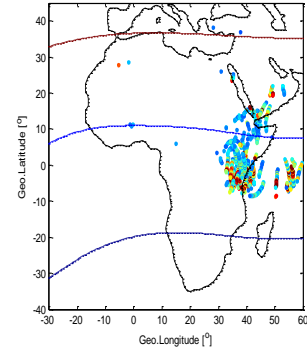
Month: March, DOY = 081  
20:00 - 23:00UT



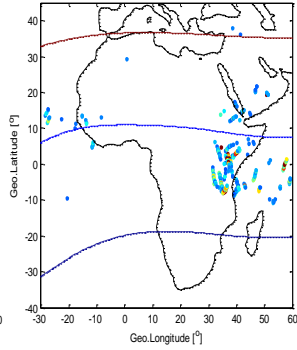
Month: March, DOY = 082  
00:00 - 04:00UT



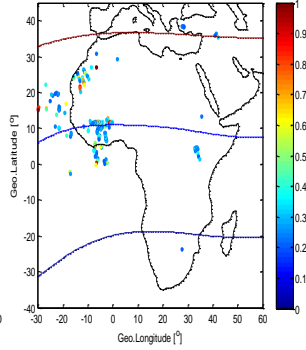
Month: March, DOY = 093  
17:00 - 20:00UT



Month: March, DOY = 093  
20:00 - 23:00UT



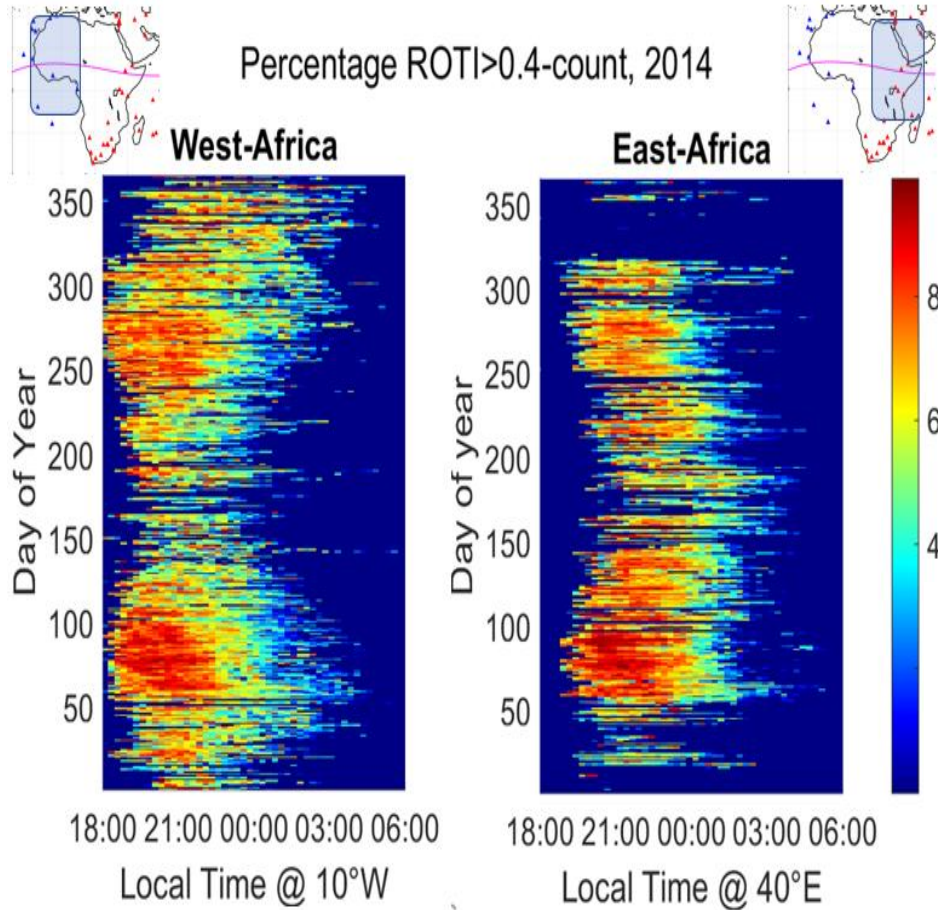
Month: March, DOY = 094  
00:00 - 04:00UT



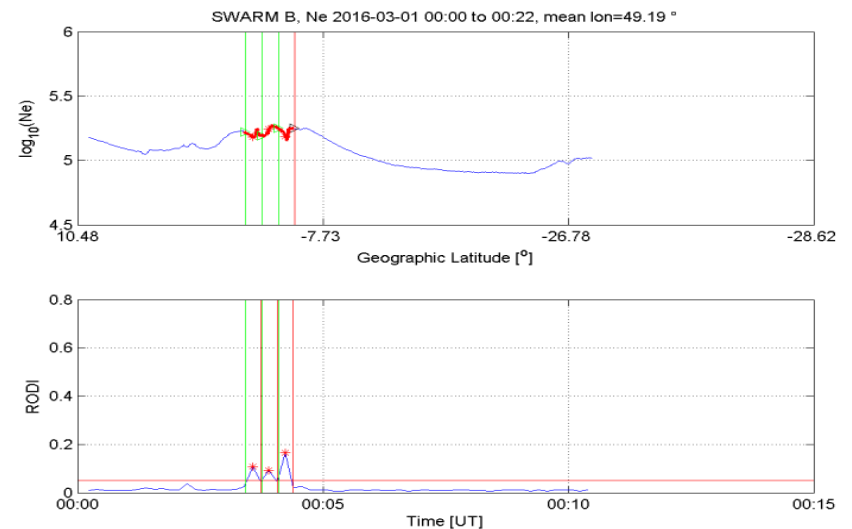
**Irregularities confined on the western side of the region with no activity on the east.**

**Irregularities confined on the East side of the region with no activity on the west.**

# Annual variability over Africa in 2014:



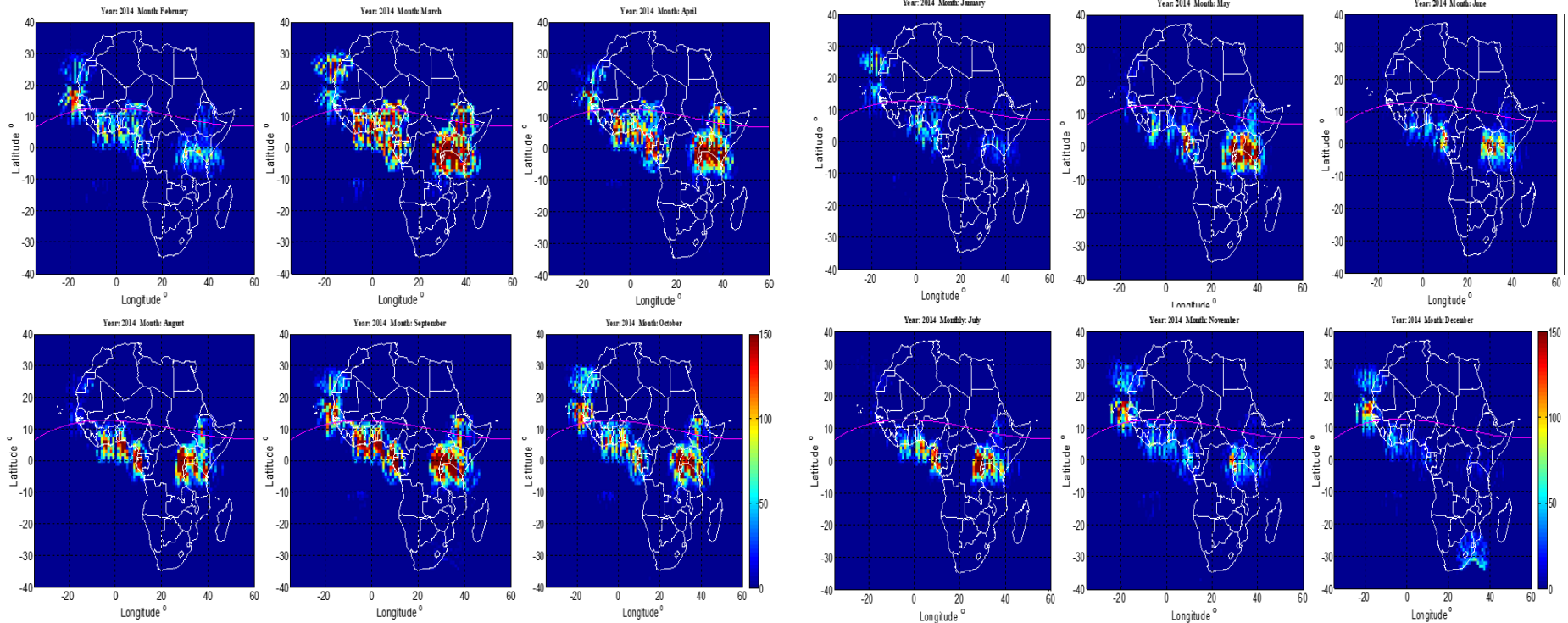
**Ionospheric irregularity activity distribution across the African region based on the percentage of ROTI counts above 0.4 for the year 2014 for stations located on the western side (on the left) and stations located to the eastern side (on the right).**



# Seasonality Across African region: Year: 2014

## Equinoxes

## Solstice

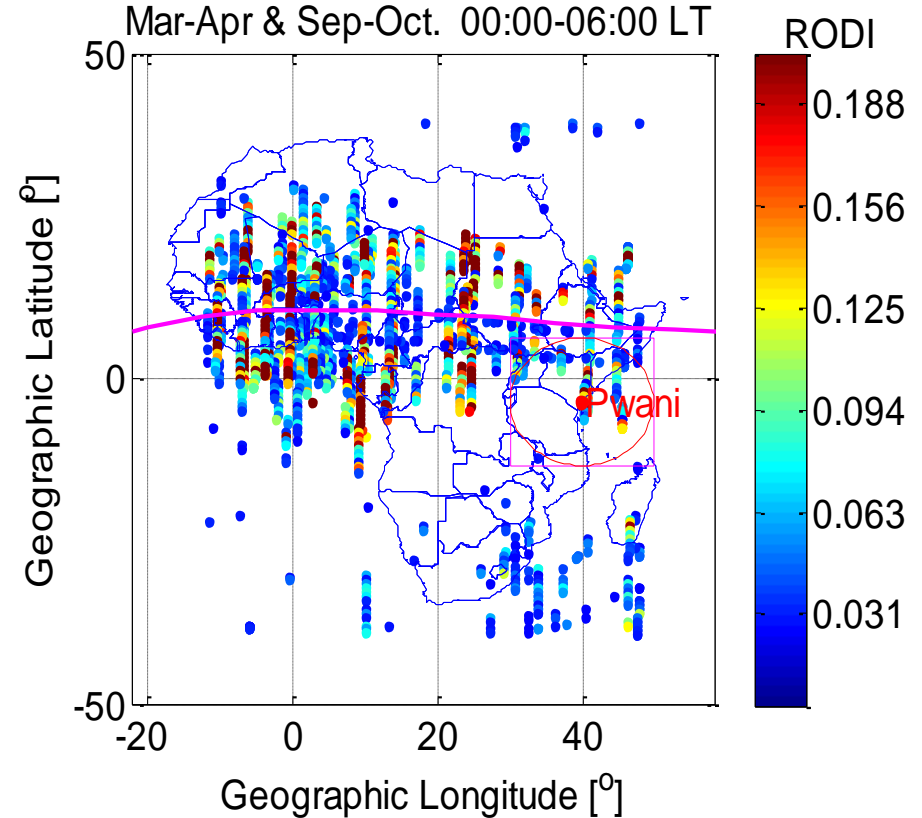
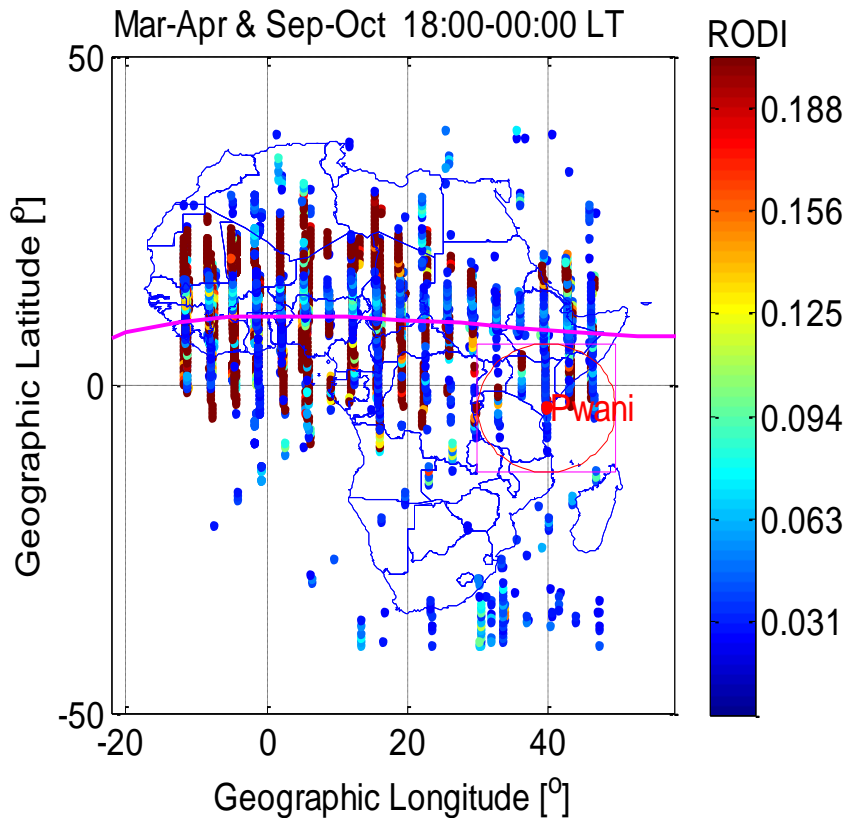


**Irregularity occurrence has a very strong seasonal dependence with enhanced Activity levels in equinoxes and reduced rates in solstices. They occur around the Year in all months.**



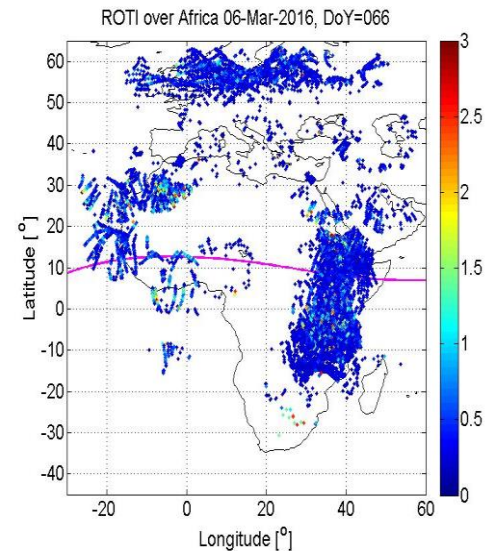
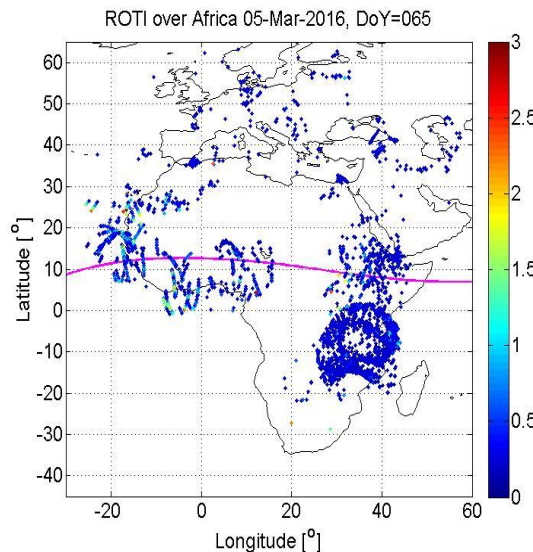
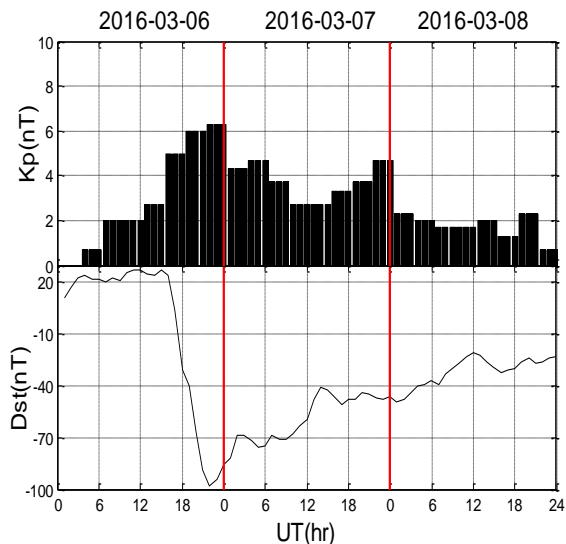
# Longitudinal Differences: Irregularity Activity

## Year:2014, SWARM B.

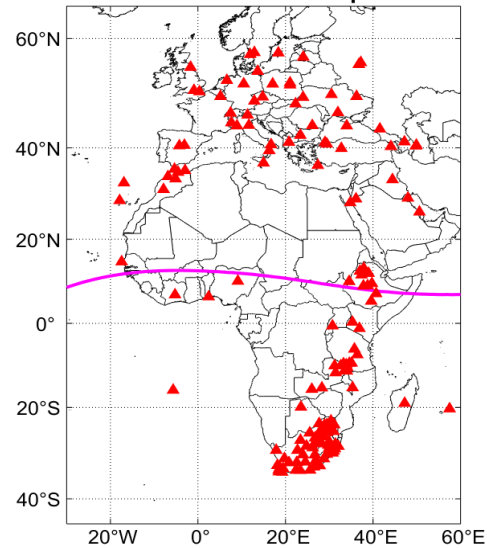


RODI is much more intense (stronger) on the Western side of the African region than on the Eastern side. More investigation is needed as to why there is more irregularity activity on the Western side.

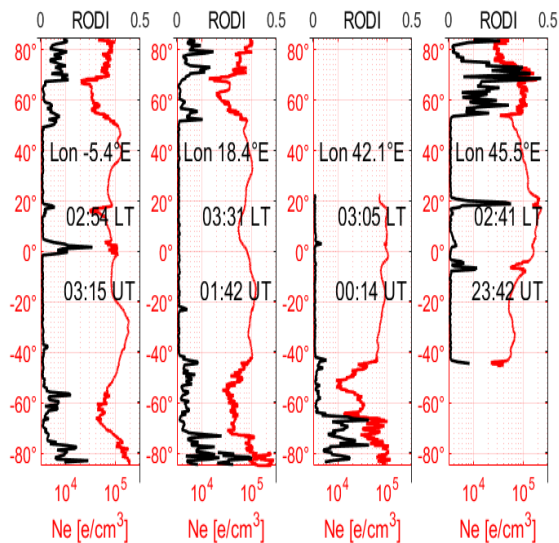
# Ionospheric Irregularities during storm: High-mid latitude Coupling



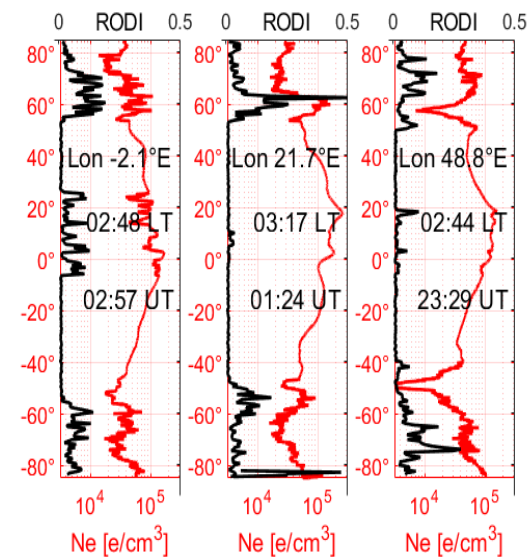
Receiver locations Africa-Europe 06-Mar-2016



From Swarm B 06-Mar-2016

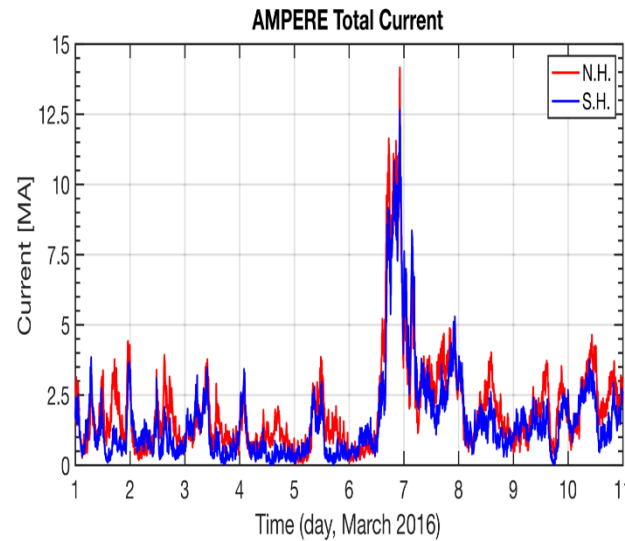
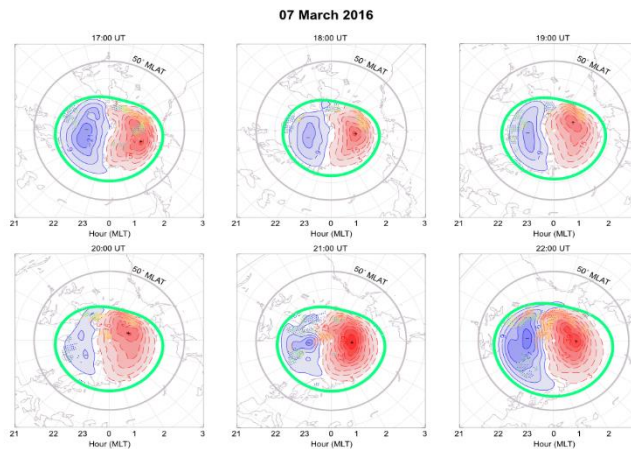
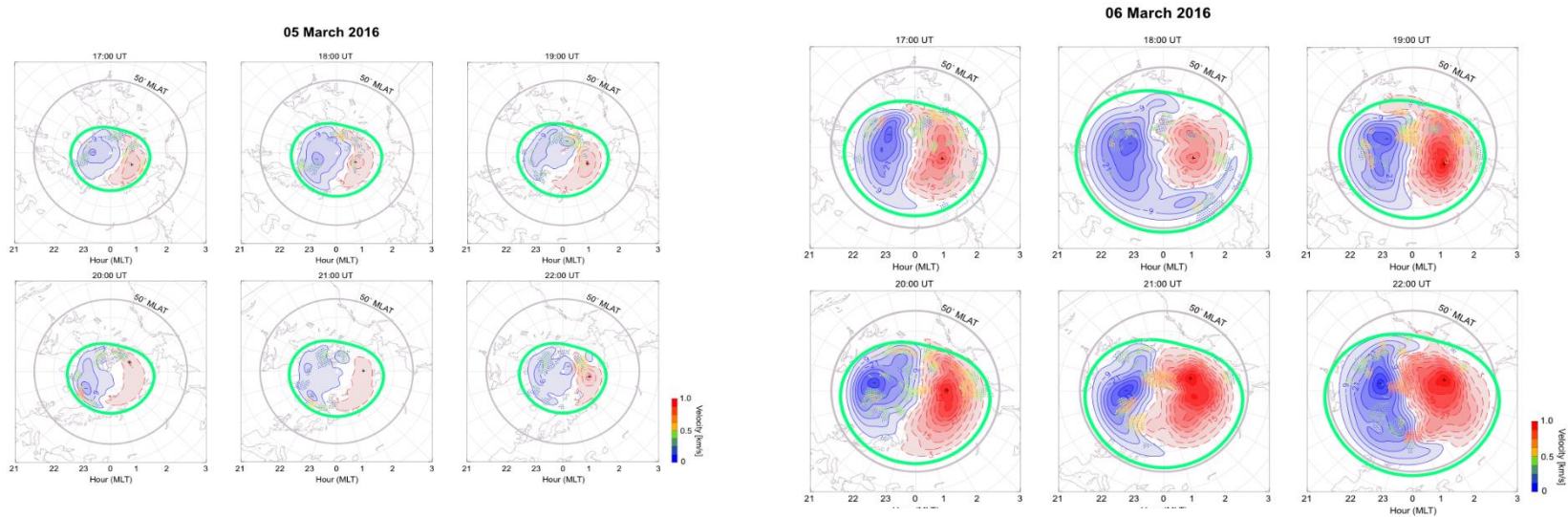


From Swarm B 07-Mar-2016



# Where did the Mid Latitude irregularities come from?

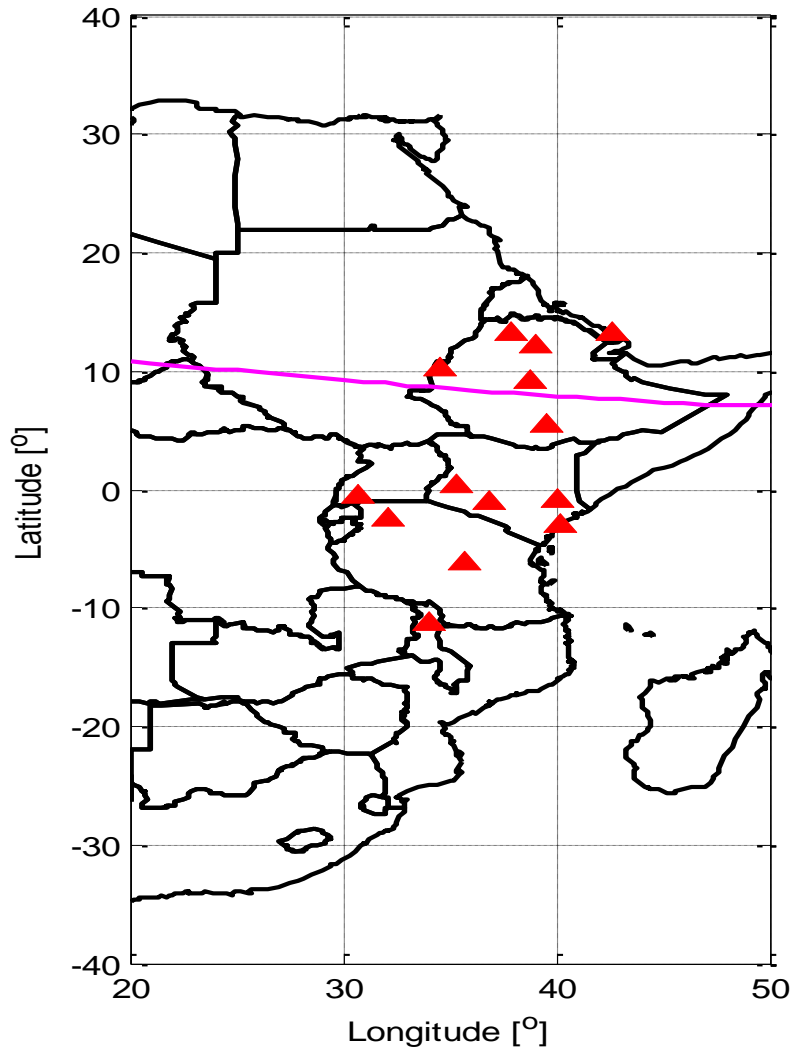
## Coupling Expansion of Auroral oval during storm



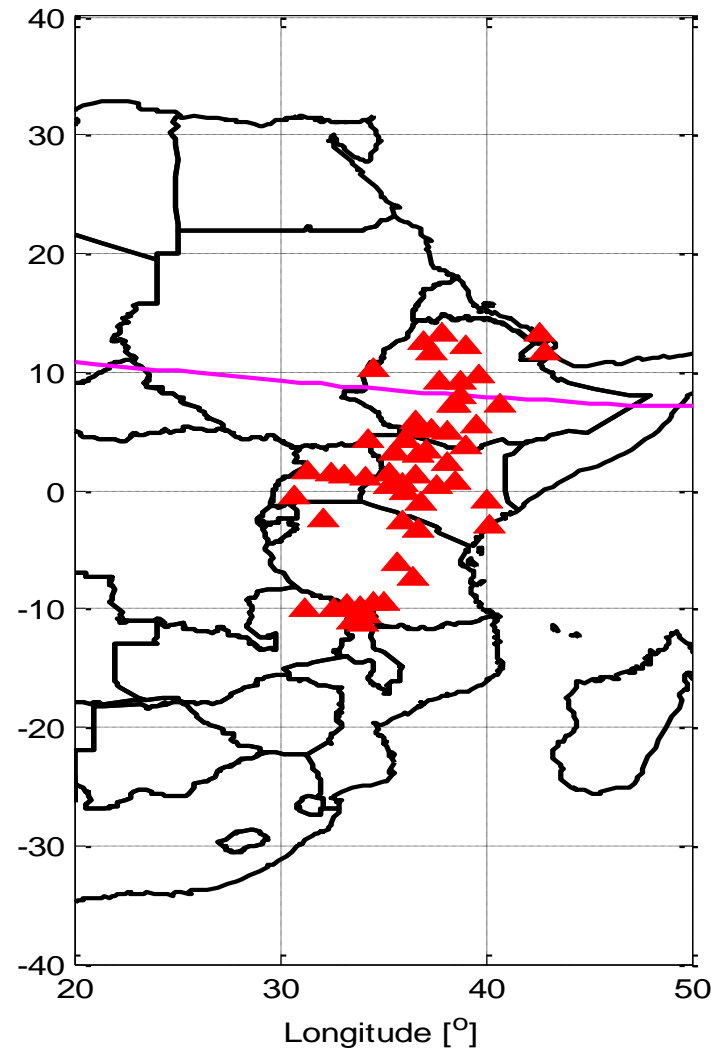
**AMPERE current intensity in the Northern Hemisphere (red) and Southern Hemisphere (blue) during the period 1–11 March 2016.**

# East African Dense Network with Potential for improved VTEC mapping

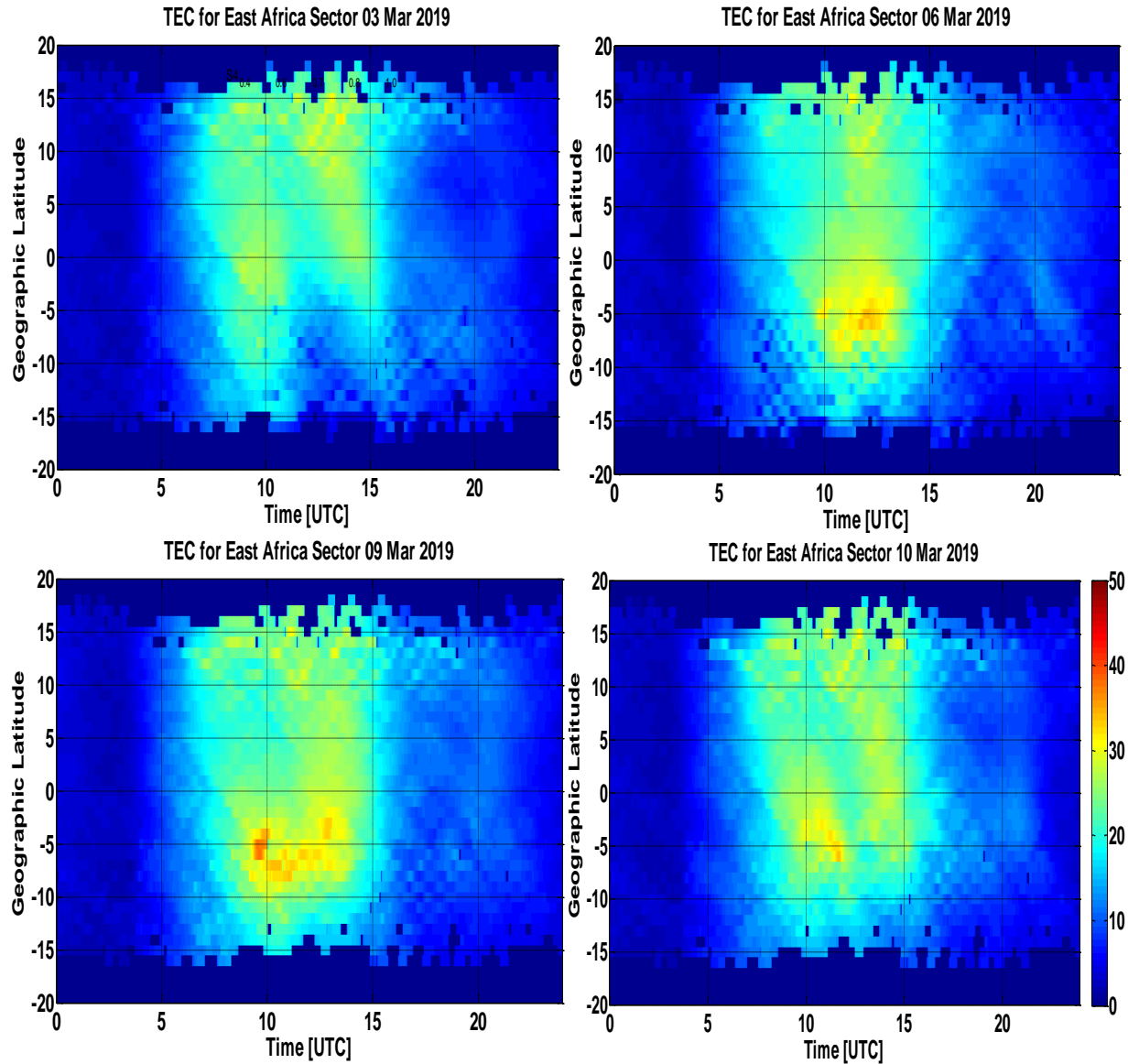
E.A IGS stations. Year: 2012



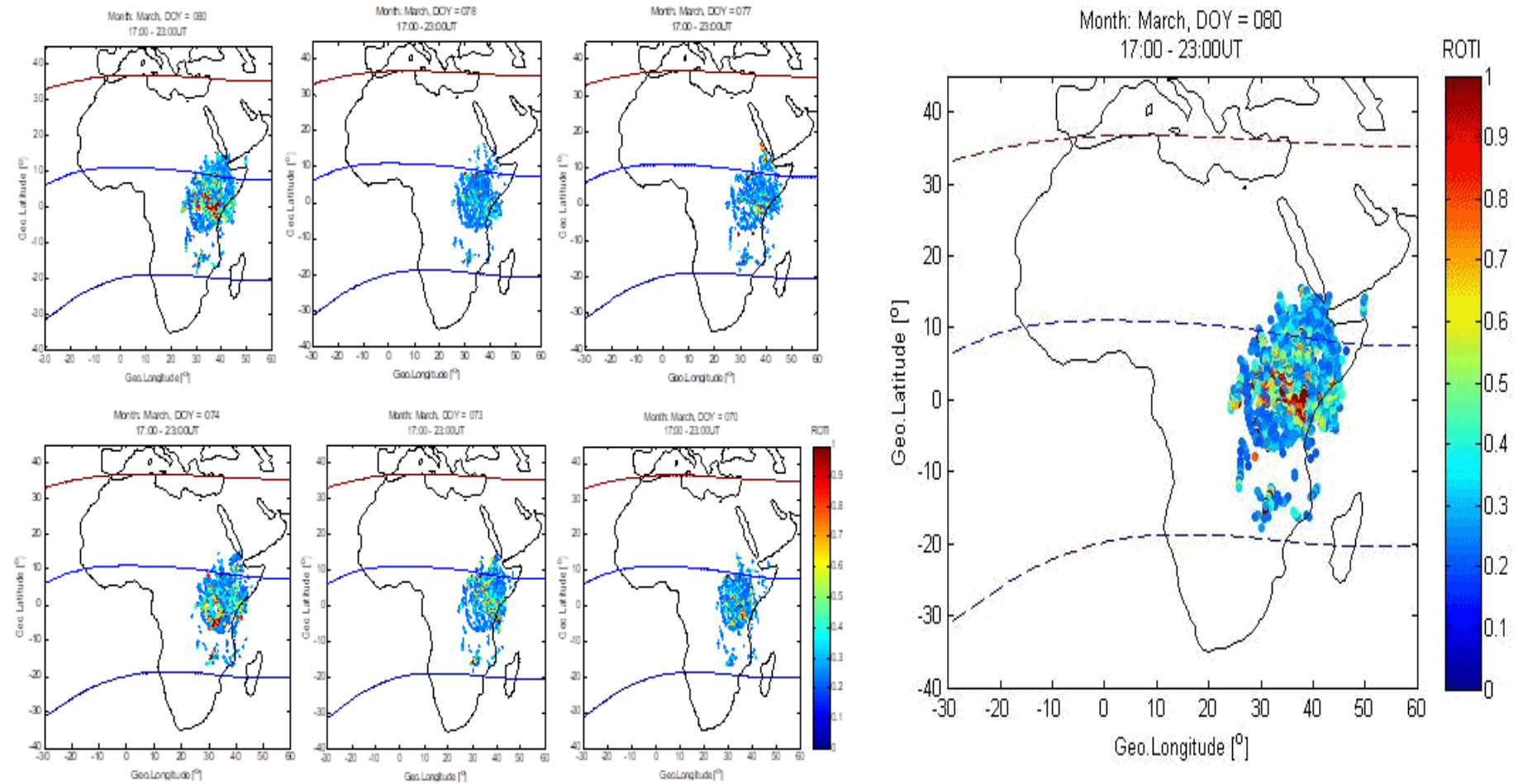
E.A IGS stations. Year: 2019



# Detailed Structuring Features of the Ionosphere over the East African sector

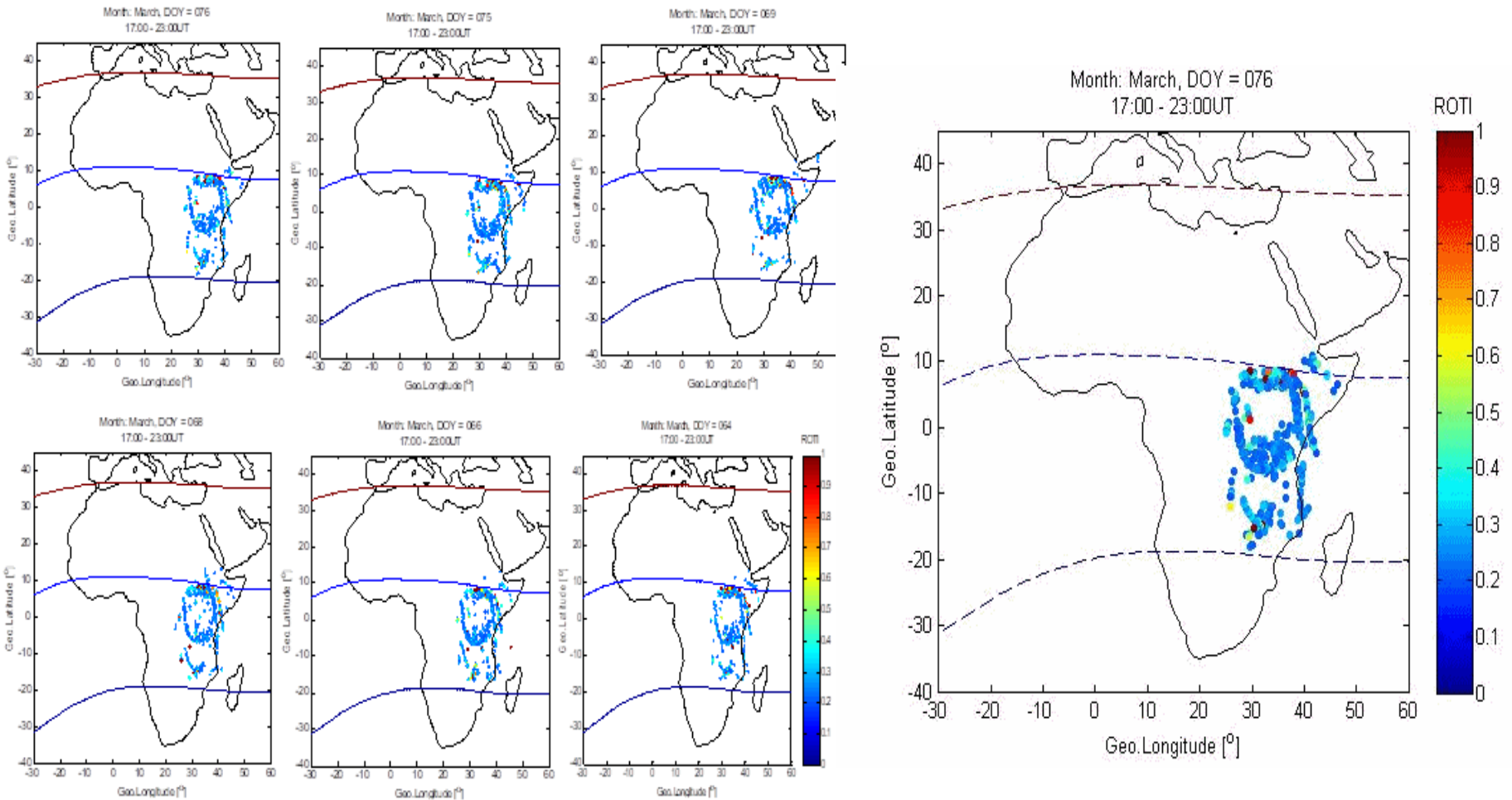


# Structuring of Irregularities from a dense network:



A dense network of receivers can give a 3-dimensional morphology of irregularities when viewed along the ray paths from every GPS satellite to all the stations over the region.

# The inverted C-shell structure- Year of Observation: 2019



Plasma bubbles: vertically elongated wedges of depleted plasma that drift upward then eastward/dip equator and downwards towards the southern hemisphere followed by an inward inverted C structure towards the west and toward the dip equator. **END**

# Summary on Irregularities at the low latitude

The general features of the irregularities are:

- Plasma irregularities generally occur after ~20:00 LT and continue for about an hour to several hours and sometimes until sunrise.
- Post-sunset irregularities are frequent, intense and last longer centered around the magnetic equator at equinoxes especially at high solar activity.
- The irregularities usually start appearing in the bottom-side ionosphere when it raises above a threshold height that varies with various geophysical conditions.
- The irregularities quickly rise to high altitudes well beyond the ionospheric peak, sometimes rising beyond 2000 km at the equator.
- As the irregularities rise in altitude, they move poleward aligned along the geomagnetic field lines, covering up to  $\pm 30^\circ$  magnetic latitudes in extreme cases.
- The irregularities usually drift eastward with velocity in the range of 100 to 200 m/s.
- Geomagnetic activity intensifies the irregularities in some cases and inhibits them in other cases.



## References:

- Hargreaves, J. K., Auroral absorption of HF radio waves in the ionosphere: a review of results from the first decade of riometry(1969), Proc. IEEE, 57, 1348-1373, 1969.
- Olsen, N., C. Stolle, R. Floberghagen, G. Hulot, A. Kuvshinov, (2016), Special issue 'Swarm science results after 2 years in Space', Earth, Planets and Space, 68:172, doi:10.1186/s40623-016-0546-6.
  - Olowendo, O. J., et al., (2012), Using GPS-SCINDA observations to study the correlation between scintillation, total electron content enhancement and depletion over the Kenya region. Adv. Space Res., 49, 1363-1372, doi:10.1016/j.asr.2012.02.006.
  - Olowendo, O. J., et al., (2016), Low latitude ionospheric scintillation and zonal plasma irregularity drifts climatology around the equatorial anomaly crest over Kenya. J. Atmos. Sol.- Terr. Phys., 138-139, 9-22.
  - Park, J., et al., (2005), Global distribution of equatorial plasma bubbles in the pre-midnight sector during solar maximum as observed by KOMPSAT-1 and Defense meteorological Satellite Program F15, J. Geophys. Res., 110, A07308.
  - Paznukhov, V. V., et al., (2012) Equatorial plasma bubbles and L-band scintillations in Africa during solar minimum. Ann. Geophys., 30, 675-682.
  - Pi., X., Mannucci, A.J., Lindqwister, U.J., and C.M. Ho., *Geophys. Res. Lett.*, 24, 2283, 1997.
  - Yizengaw, E., et al., (2013), Post-midnight bubbles and scintillation in the quiet-time June solstice. Geophys. Res. Lett. 40, 5592-5597.
  - Zakharenkova, I., and E. Astafyeva (2015), Topside ionospheric irregularities as seen from multisatellite observations. J. Geophys. Res. Space Physics 120, 807-824.